NUREG/IA–0195

International Agreement Report

LBLOCA Analysis in a Westinghouse PWR 3-Loop Design Using RELAP5/MOD3

Prepared by

J.I. Sánchez, C.A. Lage, T. Núñez

Empresa Nacional del Uranio S.A.
Santiago Rusinol, 12
28040 Madrid
SPAIN

Office of Nuclear Regulatory Research
U.S. Nuclear Regulatory Commission
Washington, DC 20555–0001

January 2001

Prepared as part of
The Agreement on Research Participation and Technical Exchange
under the International Code Application and Maintenance Program (CAMP)

Published by
U.S. Nuclear Regulatory Commission

AVAILABILITY OF REFERENCE MATERIALS IN NRC PUBLICATIONS

NRC Reference Material

As of November 1999, you may electronically access NUREG-series publications and other NRC records at NRC's Public Electronic Reading Room at www.nrc.gov/NRC/ADAMS/index.html.
Publicly released records include, to name a few, NUREG-series publications; *Federal Register* notices; applicant, licensee, and vendor documents and correspondence; NRC correspondence and internal memoranda; bulletins and information notices; inspection and investigative reports; licensee event reports; and Commission papers and their attachments.

NRC publications in the NUREG series, NRC regulations, and *Title 10, Energy*, in the Code of *Federal Regulations* may also be purchased from one of these two sources.

1. The Superintendent of Documents
   U.S. Government Printing Office
   P. O. Box 37082
   Washington, DC 20402–9328
   www.access.gpo.gov/su_docs
   202–512–1800
2. The National Technical Information Service
   Springfield, VA 22161–0002
   www.ntis.gov
   1–800–533–6847 or, locally, 703–805–6000

A single copy of each NRC draft report for comment is available free, to the extent of supply, upon written request as follows:
Address: Office of the Chief Information Officer,
Reproduction and Distribution
Services Section
U.S. Nuclear Regulatory Commission
Washington, DC 20555-0001
E-mail: DISTRIBUTION@nrc.gov
Facsimile: 301–415–2289

Some publications in the NUREG series that are posted at NRC's Web site address www.nrc.gov/NRC/NUREGS/indexnum.html are updated periodically and may differ from the last printed version. Although references to material found on a Web site bear the date the material was accessed, the material available on the date cited may subsequently be removed from the site.

Non-NRC Reference Material

Documents available from public and special technical libraries include all open literature items, such as books, journal articles, and transactions, *Federal Register* notices, Federal and State legislation, and congressional reports. Such documents as theses, dissertations, foreign reports and translations, and non-NRC conference proceedings may be purchased from their sponsoring organization.

Copies of industry codes and standards used in a substantive manner in the NRC regulatory process are maintained at—
The NRC Technical Library
Two White Flint North
11545 Rockville Pike
Rockville, MD 20852–2738

These standards are available in the library for reference use by the public. Codes and standards are usually copyrighted and may be purchased from the originating organization or, if they are American National Standards, from—
American National Standards Institute
11 West 42nd Street
New York, NY 10036–8002
www.ansi.org
212–642–4900

The NUREG series comprises (1) technical and administrative reports and books prepared by the staff (NUREG–XXXX) or agency contractors (NUREG/CR–XXXX), (2) proceedings of conferences (NUREG/CP–XXXX), (3) reports resulting from international agreements (NUREG/IA–XXXX), (4) brochures (NUREG/BR–XXXX), and (5) compilations of legal decisions and orders of the Commission and Atomic and Safety Licensing Boards and of Directors' decisions under Section 2.206 of NRC's regulations (NUREG–0750).

NUREG/IA-0195

International Agreement Report

LBLOCA Analysis in a Westinghouse PWR 3-Loop Design Using RELAP5/MOD3

Prepared by

J.I. Sánchez, C.A. Lage, T. Núñez

Empresa Nacional del Uranio S.A.
Santiago Rusinol, 12
28040 Madrid
SPAIN

Office of Nuclear Regulatory Research
U.S. Nuclear Regulatory Commission
Washington, DC 20555-0001

January 2001

Prepared as part of
The Agreement on Research Participation and Technical Exchange
under the International Code Application and Maintenance Program (CAMP)

Published by
U.S. Nuclear Regulatory Commission

ABSTRACT.

This report documents the analysis of a postulated Large Break Loss-of-Coolant Accident (LBLOCA) in a Westinghouse 3-Loop PWR design analysed using the "Best Estimate" code RELAP5/MOD3. This LBLOCA calculation represents ENUSA's contribution to the "Code Assessment and Maintenance Program" (CAMP).

The code used for this analysis is RELAP5/MOD3.2 - the latest CAMP version that was available to ENUSA when this study was performed. Nevertheless, since this version lacked of a reflood axial mesh renoding model, a developmental version was also used to analyse the reflood portion of the accident. This developmental version is RELAP5/MOD3.2 fg.

Five calculations were analysed, and the results of these were compared. The first case described in this document compares two runs made, using the same input deck, on two different platforms: the CRAY-YMP, and the ALPHA SERVER 4100. Both calculations were done with a basic nodalization: downcomer modelled with one 1-D component (collapsed downcomer), without the gap conductance model, and without the reflood model. Both cases were run with the original RELAP5/MOD3.2 version.

The second case was run to check the impact of modelling a quasi-three-dimensional downcomer, modelled with three 1-D components joined with cross-flow junctions. For this case, the base nodalization used in the first case was modified by adding the new downcomer model, and then compared with the previous results. This case was run on the ALPHA SERVER 4100 with version RELAP5/MOD3.2.

Finally, for the third case analysed, two additional input decks were prepared. Both of these included the three-dimensional downcomer nodalization and the gap conductance model. The first calculation was done with RELAP5/MOD3.2 with its standard heat transfer package. The second calculation was done with the reflood model activated, and using the developmental version RELAP5/MOD3.2 fg.

The first case analysed showed minimal differences between the results obtained on the two platforms used. The second case analysed showed the impact of the downcomer nodalization and the three-dimensional effects are shown to be non-negligible. The third case analysed clearly shows the need for a specific reflood model for this kind of transient, instead of the standard heat transfer package. The standard heat transfer package produces a very oscillatory behavior under reflooding conditions.

INDEX OF CONTENTS

INDEX OF TABLES

INDEX OF FIGURES

INDEX OF FIGURES

EXECUTIVE SUMMARY

This report documents the analysis of a postulated Large Break Loss-of-Coolant Accident (LBLOCA) in a Westinghouse 3-Loop PWR design analysed using the "Best Estimate" code RELAP5/MOD3. This LBLOCA calculation represents ENUSA's contribution to the "Code Assessment and Maintenance Program" (CAMP).

The code used for this analysis is RELAP5/MOD3.2 - the latest CAMP version that was available to ENUSA when this study was performed. Nevertheless, since this version lacked a reflood axial mesh renoding model, a developmental version was also used to analyse the reflood portion of the accident. This developmental version is RELAP5/MOD3.2 fg.

Five calculations were done, and the results of these compared. The first case described in this document compares two runs made, using the same input deck, on two different platforms: the CRAY-YMP, and the ALPHA SERVER 4100. Both calculations were done with a basic nodalization: downcomer modelled with one 1-D component (collapsed downcomer), without the gap conductance model, and without the reflood model. Both cases were run with the RELAP5/MOD3.2 version. Minimal differences between the results obtained in both machines have been showed.

The second case run was to check the impact of modelling a quasi-three-dimensional downcomer (modelled with three 1-D components joined with cross-flow junctions). For this case, the basic nodalization used in the first case was modified by adding the new downcomer model, and then compared with the previous results. This case was run on the ALPHA SERVER 4100 with version RELAP5/MOD3.2. This case show a non-negligible impact of the downcomer nodalization on the ECCS bypass phenomenon. The quasi-three-dimensional approximation reduces the ECCS bypass and, consequently, the core recovery in the reflood period begins earlier.

Finally, for the third case analysed, two additional input decks were prepared. Both of these included the three-dimensional downcomer nodalization and the gap conductance model. The first calculation was done with RELAP5/MOD3.2 with its standard heat transfer package. The second calculation was done with the reflood model activated, and using the developmental version RELAP5/MOD3.2 fg. The results with the heat transfer package show a oscillatory behaviour when compared with the reflood model calculation.

Due to the highly dependence of the downcomer model in this accident, where 3-D phenomena are very important, further work is considered necessary to assess the capability of RELAP5/MOD3.2 to model this accident.

All cases analyzed show ample margin to the 10CFR50.46 limits. That is, the peak cladding temperature (PCT) is well bellow 2200 ºF, the maximum local oxidation is well bellow 17 % of the initial cladding thickness, and the overall hydrogen generation is well bellow 1%. A coolable core geometry is maintained, and long term cooling of the core is assured.

1. INTRODUCTION.

This report documents the "best estimate" code RELAP5/MOD3 studies done by ENUSA as the "in kind" contribution to the "Code-Assessment and Maintenance Program" (CAMP). Taking as basis the simulation of a Large Break Loss of Coolant Accident (LBLOCA) for a Spanish 3-loop PWR, the study considered the different aspects and scope that are indicated next:

- To verify the effect of the downcomer nodalization in a LBLOCA study, in which three-dimensional phenomena are expected to be important.
- To verify the gap conductance model during the steady state calculation, by comparison against results from the steady-state fuel rod design codes used at ENUSA.
- To compare the results obtained with the standard heat transfer package and the new reflood model under reflooding conditions (the latter available in the 3.2fg version).
- To check the code performance for a given analysis, using two different computer platforms on which the code is currently installed at ENUSA.

The plant selected for this LBLOCA analysis is a typical three-loop Westinghouse 17x17 fueled PWR design.

RELAP5/MOD3 was developed at the Idaho National Engineering Laboratory (INEL) for the U. S. Nuclear Regulatory Commission (USNRC). The code version in this study is RELAP5/MOD3.2, the latest version released under the CAMP program at the time of this study.

The postulated accident consists in a 200% double-ended guillotine break in the cold leg, which is considered a design-basis accident in licensing applications. It must be demonstrated from the analysis that the Emergency Core Cooling System (ECCS) provides sufficient protection to keep the core below the limits that are defined in the 10CFR50.46 regulation.

Chapter 2 provides a description of the reactor and describes the postulated accident scenario analysed in this study. Chapter 3 describes briefly both the standard and developmental code versions used for this study. Chapter 4 describes the base case (first case) calculation on the two different computer platforms (CRAY-YMP and ALPHA-SERVER 4100). A sensitivity analysis considering three-dimensional effects in the downcomer during the blowdown phase is documented in Chapter 5 (second case). The performance of the dynamic gap conductance and clad deformation models, and a comparison of the standard heat transfer package and the reflood model is included in Chapter 6 (third case). Since the as-released RELAP5/MOD3 version 3.2 does not include a fine mesh reflood capability, a new version of the code having this capability was requested from the USNRC. This version, still under development, is the 3.2fg

version which was used for the third case analysed. Finally, run statistics are given in Chapter 7. Finally, summary and main conclusion are given in chapter 8.

2. PLANT DESCRIPTION AND SCENARIO.

The plant analysed is a 3-Loop PWR of Westinghouse design, with a rated power of 2686 MWth and a thermal design flow rate of 270,000 gpm. The core is composed of 157 fuel assemblies of the 17x17 lattice design and has an active fuel height of 12 feet.

The accident scenario consists of a LBLOCA 200% double-ended guillotine break located in the cold leg in the loop to which the pressurizer surge line is connected. This break location and size produces the most limiting results in the safety analysis for this reactor. At the time of the break, loss of offsite power is assumed with the reactor operating at 100% rated power.

For this transient, the depressurization of the reactor coolant system (RCS) produces a pressure decrease in the pressurizer until the reactor trip signal is reached. The ECCS is subsequently activated when this low pressure trip setpoint is reached.

In the initial stages of the transient, the core is covered with subcooled liquid, and the heat transfer between the fuel rod wall and the coolant is provided by the mechanism of forced convection, with some nucleate boiling. Very early in the transient, departure from nucleate boiling is reached, at which point the heat transfer becomes very unstable and a sudden increase in cladding temperature is experienced, due mainly to the redistribution of the internal stored energy in the fuel.

When the primary pressure drops below the accumulators pressure, subcooled water from the accumulator enters the pressure vessel. Part of this water, however, is lost through the break to the containment building.

The blowdown phase ends when the pressure in the primary system reaches the pressure of the containment building. Water discharged from the accumulators begins to replenish the pressure vessel lower head and lower plenum, and reaches the bottom of the core. This represents the beginning of the reflood phase.

The downcomer water column provides the driving force needed to reflood the core and return the cladding temperature to saturation. The ECCS continues refilling the downcomer to maintain the pressure vessel water inventory.

Table 1 summarises important input parameters and the initial conditions at the beginning of the transient that were assumed in the calculations. Although RELAP5/MOD3 is a best-estimate code, some conservative assumptions in the initial and boundary conditions were made in the calculations. These assumptions are listed below:

- Peaking factors at the maximum values specified in the plant's Technical Specifications.
- Chopped Cosine Axial Power Shape.
- Maximum stored energy in the fuel rods (only in the third case analysed; see Chapter 6).
- Decay power taken to be 120% of the 1971 ANS standard.
- Constant Containment Pressure at 1 bar.
- Single failure criterion for the ECCS assumed (the failure of one diesel engine precludes the actuation of two of the three safety injection pumps).
- Conservative delays in the ECCS actuation assumed (25 seconds).
- Reactor coolant pumps tripped at the beginning of the transient.
- ECCS in Broken loop not modelled.

Table 1 . Initial Conditions and Relevant Input Parameters

Core Power	100% of 2686 Mwt
Peak linear Power	12.9 kw/ft
Total Core Peaking Factor F_Q^T	2.40
Core Axial Power Shape	Chopped Cosine
Hot Assembly Average Rod Radial Peaking Factor $F_{\Delta H}$	1.60
Fuel Type Analyzed	17x17
Rod Internal Pressure	7.29 Mpa
Secondary Steam Pressure	6.72 Mpa
Steam Generator Tube Plugging Level	0 %
Initial Loop Mass Flow Rate	4416 kg/sec.
Number of LHSI/HHSI Pumps Running	1
Assumed Delay for full Safety Injection Flow	25 sec.
Accumulator Tank Volume	41.05 m^3
Accumulator Water Volume	27.6 m^3
Accumulator Water Temperature	305 K
Barrel-Baffle Configuration	Up-flow

3. CODE VERSION AND NODALIZATION.

The code version used in this study is RELAP5/MOD3.2, the latest version officially released under the CAMP agreement at the time of this study.

Since the as-released RELAP5/MOD3.2 does not include a fine mesh reflood capability, a new version of the code was requested from the USNRC. This version is the 3.2fg version (Internal INEL name), a developmental version of RELAP5 that includes the modifications made in the Mod3.2.1.2 version, and the updates made since April 1996, plus a fix for reflood memory and the Paul Scherrer Institute (PSI) reflood model (Ref. 1). This version was used for the reflood sensitivity studies (third case analysed).

The nodalization diagram is shown in Figures 1 and 2. This nodalization follows the general recommendations given in the RELAP user's guide for this kind of analysis (Ref. 2).

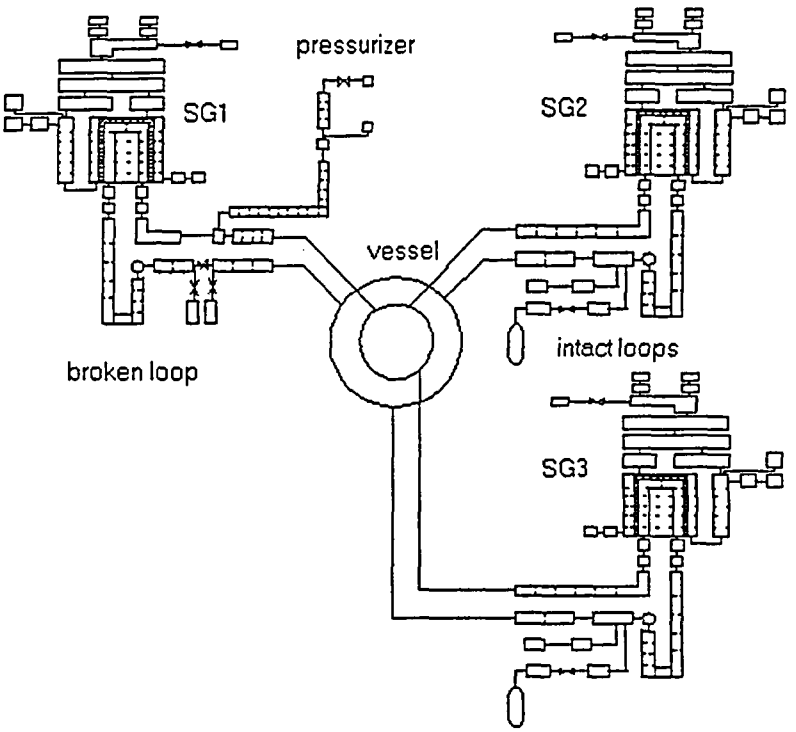

Figure 1. Three Loops Nodalization

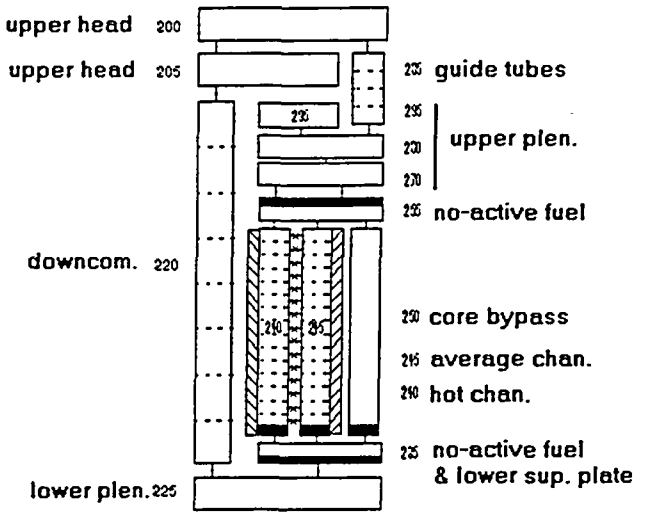

Figure 2. Vessel Nodalization (collap. downcomer).

The final nodalization scheme used the following groupings of components, in which the three coolant loops were modelled explicitly:

- The primary side was modelled with 219 hydrodynamic volumes (241 in the three-dimensional downcomer case), and 233 junctions (284 in the three-dimensional downcomer case).

- The secondary side contains 51 hydrodynamic volumes and 57 junctions.

- The number of heat structures are 81 and the total number of mesh points used are 558.

The detail of this nodalization and the maximum time step selected (0.05 seconds during the blowdown period and 0.0125 sec. during the reflood period) are considered to be fine enough to give an accurate and stable solution for a LBLOCA transient.

The following nodalization numbering scheme was used:

- Components 200 to 295 to model the reactor vessel.
- Components 10 to 13 to model the broken loop, including the pressurizer surge line.
- Components 40 to 43 to model the pressurizer
- Components 14 to 38 to model the intact loops
- Components 110 to 130 to model the steam generators (primary side)
- Components 500 to 912 to model the steam generators (secondary side)

A brief description of the nodalization is given below.

Reactor Vessel

The reactor pressure vessel consists of the vessel wall, downcomer, core barrel, lower head, inlet plenum and internals, the core, upper plenum and internals, the guide tubes and support columns, and the upper head. The vessel is modelled using several components to describe the multiple flowpaths inside the vessel (see Fig. 2).

The downcomer was modelled with an "annulus" component with 8 axial nodes. In the three-dimensional downcomer model, three "annulus" components were modelled with three multiple cross flow junction components. Three "sngljun" components connect the downcomer with each separate cold leg. The lower head is modelled with a single "branch" component. Another "branch" component is used to model the lower plenum up to the elevation where the active fuel portion of the core begins.

The core is divided in two regions: the first, representative of the average power zone with 148 fuel assemblies, and the second operating at a higher power and comprised of 9 fuel assemblies. Both regions are modelled with "pipe" components of 15 axial cells, interconnected to model crossflow paths with a "mtpljun" component. With this nodalization the hot channel is reasonably modelled and the hot channel/average channel core volumes maintain a ratio of 1/16 (in accordance with rules of Ref. 2).

Three 15 axial nodes heat structures are modelled to represent the average fuel rod in the average power region (39,072 rods). Another rod is modelled to represent the average fuel rod in the high power region (2,375 rods) with a rod power 1.125 times below the hot rod power. Finally, a single 104 kW hot rod (the hot assembly average rod radial peaking factor $F_{\Delta H}$ is 1.60). All rods are modelled with a chopped cosine axial power shape with an axial peaking factor (F^N_z) equal to 1.50. The fuel rod was modelled with ten radial mesh points to represent the different constitutive materials in the rod. A parabolic radial flux depression profile, representative of beginning of life conditions, was assumed. For the first and second cases, which were not run with the gap conductance model, an average pellet temperature of 1243 K was obtained. For the third case analysed (comparison of the reflood model and the standard heat transfer package), run with the conductance gap model, the average pellet temperature obtained was 1454 K, in good agreement with results from ENUSA's steady-state fuel performance codes.

A core bypass flow path was modelled between the lower and upper plena with a single cell "pipe" component. The bypass flow is about 4.5% of the total core flow in steady state conditions.

The upper plenum was modelled with 2 "branch" components and 1 "snglvol" component. The CCFL model was used, with the appropriate parameters for this geometry in the upper plenum.

The upper guide tubes were modelled with a four cell "pipe" component that connects the upper plenum region with the upper head.

The upper head was modelled with two branch components.

Primary Loops.

Each of the three loops was modelled separately, including the hot leg, the pressurizer and surge line, the steam generator, the reactor coolant pump, the cross-over leg, cold

leg and the accumulator tanks. The ECCS was modelled as a boundary condition (time dependent junctions).

Hot Leg

The hot leg for the intact loops was modelled with "pipe" components with a total of six cells. The hot leg in the broken loop was also modelled with a total of six cells, but using three components: two "branch" components and a central "pipe" component where the pressurizer surge line is connected. The hot leg elbow to the steam generator plenum using the CCFL option has been explicitly modelled.

Pressurizer and Surge Line

The pressurizer, connected to the broken loop through the surge line, was modelled with one 4 cells "pipe" component for the top section of the pressurizer, and one "branch" component for the bottom section of the pressurizer.

The surge line was modelled with one "pipe" component with a total of 15 cells.

A suitable control logic was included in the model to reach the desired initial pressurizer water level and initial pressure.

Steam Generator

- Primary Side.

Five components were used to represent the primary side of each steam generator. Four "branch" components were used to model the inlet and outlet steam generator chambers. The CCFL option, with the constant parameters representative of this geometry, was used in the connection of the inlet plenum with the steam generator tubes. A single tube, representing the whole tube bundle, was modelled using a "pipe" component with 12 cells.

- Secondary Side.

Up to 23 components were used to model the secondary side of each steam generator and the steam lines, including the suitable elements to adjust the downcomer level at the desired value.

The boiler was simulated with a "pipe" component with 6 cells. The bundle option was selected. Hydraulic diameters were calculated and included in the input deck to allow the code to properly determine the interfacial drag.

The transition region from the boiler to the separator was modelled with a branch component.

The primary separators were modelled using the RELAP separator component.

The steam dome was modelled with a branch component.

The steam generator downcomer was modelled with a branch component for the upper downcomer, and with an annulus component with 6 cells for the lower downcomer. In

order to get the specified circulation ratio, appropriate form loss energy coefficients were included in the downcomer and in its connection with the boiler.

Time-dependent volume, time-dependent junction and valve components were used to simulate the steam generator secondary boundary conditions (pressure and level proportional-integral controls, steam and feedwater boundary conditions) for the steady state condition and during the transient. The steam generator relief and safety valves were also modelled. The Auxiliary Feed Water System was not included in this model.

- Heat Structures

Heat structures were used to model the tube wall.

Cross-Over Leg

Each cross-over leg portion of the primary piping was modelled using a "pipe" component with 10 cells.

Reactor Coolant Pump

The Reactor Coolant Pumps (RCP's) were simulated using the RELAP "pump" components, with specific head and torque homologous curves for a Westinghouse 7000 HP one-stage centrifugal pump design.

Cold Leg

The cold legs in the intact loops were modelled with one "branch" component to which the ECCS is connected and one "pipe component" with 2 cells. The cold leg in the broken loop was modelled with two "pipe" components with 2 (pump side) and 3 cells (vessel side).

Accumulator and discharge lines

The Accumulators were simulated with the RELAP "accum" components. The Accumulator discharge surge lines were modelled with "pipe" components. A check valve connects the discharge line with the cold legs. The Accumulator in the broken cold leg was not modelled.

Break

The break was modelled with two instantaneously opening "trip valves" connected to a constant pressure "tmdpvol". Choked flow multipliers equal to 1.0 were assumed for these valves, with the homogeneous option activated, as recommended in the RELAP manuals.

4. CASE 1: COMPARISON BETWEEN CRAY-YMP and ALPHA SERVER 4100 RESULTS.

Two calculations were done, using the same input deck, on two different computer platforms and the results were compared. In this way, the effect of the machine accuracy and the code compilation method on the results could be determined.

The idea to perform these calculations arose from the CAMP May 1996 meeting in Madrid. In this meeting, some participants reported very different results, in some cases, running the same input deck on different platforms.

For this comparison case, version RELAP5/MOD3.2 was installed with the default values on both the CRAY-YMP and ALPHA SERVER 4100 platforms, and the same input deck run on both machines.

The input deck used for these calculations is the most simple one: the reflood model was not selected (it is not implemented in RELAP5/MOD3.2), a one-dimensional downcomer was modelled, and the gap conductance model was not turned on (average pellet temperature of 1243 K obtained at the hottest position).

Figs. 3 and 4 show the break flow and the integrated break flow, respectively, both on the pump side. In Figs. 5 and 6, the break flow and the integrated flow on the vessel side are shown. This mass flow rate is very high at the beginning of the transient due to the subcooled choked flow at the break location. Nevertheless, the liquid in the RCS reaches saturation conditions early in the transient, and the choked flow decreases drastically. It can be observed that the results obtained on the two computer platforms are very close to each other. The same can be said from Fig. 7 where the pressurizer pressure is plotted.

Figs. 11 and 12 show the core inlet and outlet mass flow rate, respectively. During the blowndown period of the transient, the core flows shown in Figs. 11 and 12 produce two quenchings. The first is a bottom-up quench, as can be observed in Fig. 11, which finishes approximately 10 seconds after the beginning of the transient. The second one is a top-down quench that can be observed in Fig. 12. This quench begins 10 sec. after the beginning of the transient, and finishes at t = 20 seconds. Both quench phenomena produces the characteristic two peaks in the clad temperature during the blowdown period that can be observed in Figs. 13 through 18.

Fig. 8 shows the accumulator mass flow rate. The accumulator injection begins at time (t) equals 11 seconds. The accumulator empties at t = 42 sec. Figures 9 and 10 show the core collapsed liquid level and the downcomer collapsed liquid level, respectively, (data obtained by multiplying the cell liquid fraction by the cell length). After the blowdown, the liquid level in the core begins to increase at t = 31 sec., which marks the beginning of the reflood period. It can be observed that, during the reflood period, the differences obtained on the two computer platforms increase. These differences are displayed in Figures 11 and 12 (core inlet flow and core outlet flow rate, respectively).

Figures 13 through 18 show the clad temperature at different axial positions along the hot rod (note that the core axial positions are numbered from 1 to 15, and that position 1 corresponds to the lower elevation of the active fuel region). The differences between the two platforms are found to be small and the impact in the conclusion is

null. As shown in Fig. 9, globally the amount of liquid calculated in the core is very close between the two computer platforms.

Nevertheless, the CPU time spent on both platforms differs drastically, as can be observed in Fig. 19. With the installation of the default RELAP5 version on the CRAY-YMP, the CPU time needed is near 24,000 seconds, while on the ALPHA-SERVER 4100, the CPU time is lower than 4,000 seconds. The number of time advancements were 47190 and 49388 on the CRAY-YMP and ALPHA-SERVER 4100, respectively. A summary of the run statistics for these two cases can be found in Chapter 7 . Due to the excessive CPU consumption on the CRAY-YMP, it was decided to continue this CAMP study running all cases on the ALPHA-SERVER 4100 workstation.

Table 2 shows the sequence of events during the transient, and in Table 3, the result analysis for this first case is included. The local oxidation and the burst location are not calculated, because the gap conductance and oxidation models were not used.

Table 2. Sequence of Events (Case 1)

	CRAY-YMP run	ALPHA-SERVER run
Reactor trip signal	2.0 sec.	2.0 sec.
SI signal generated	3.0 sec.	3.0 sec.
Accumulator injection	11 sec.	11 sec.
End of bypass	19 sec.	19 sec.
End of blowdown	26 sec.	26 sec.
Safety injection	26 sec.	26 sec.
Beginning of reflood	31 sec.	31 sec.
Accumulator empties	42 sec.	42 sec.

Table 3. Analysis of Results (Case 1)

	CRAY-YMP run	ALPHA-SERVER run
Peak clad temperature	1140 K	1125 K
Time of peak clad temp.	31 sec.	31 sec.
Peak clad temp. elevation	1.9512 m	1.9512 m
Local oxidation	-	-
Hot rod burst time	-	-
Hot rod burst location	-	-

Figure 3. Break Mass Flow (pump side)

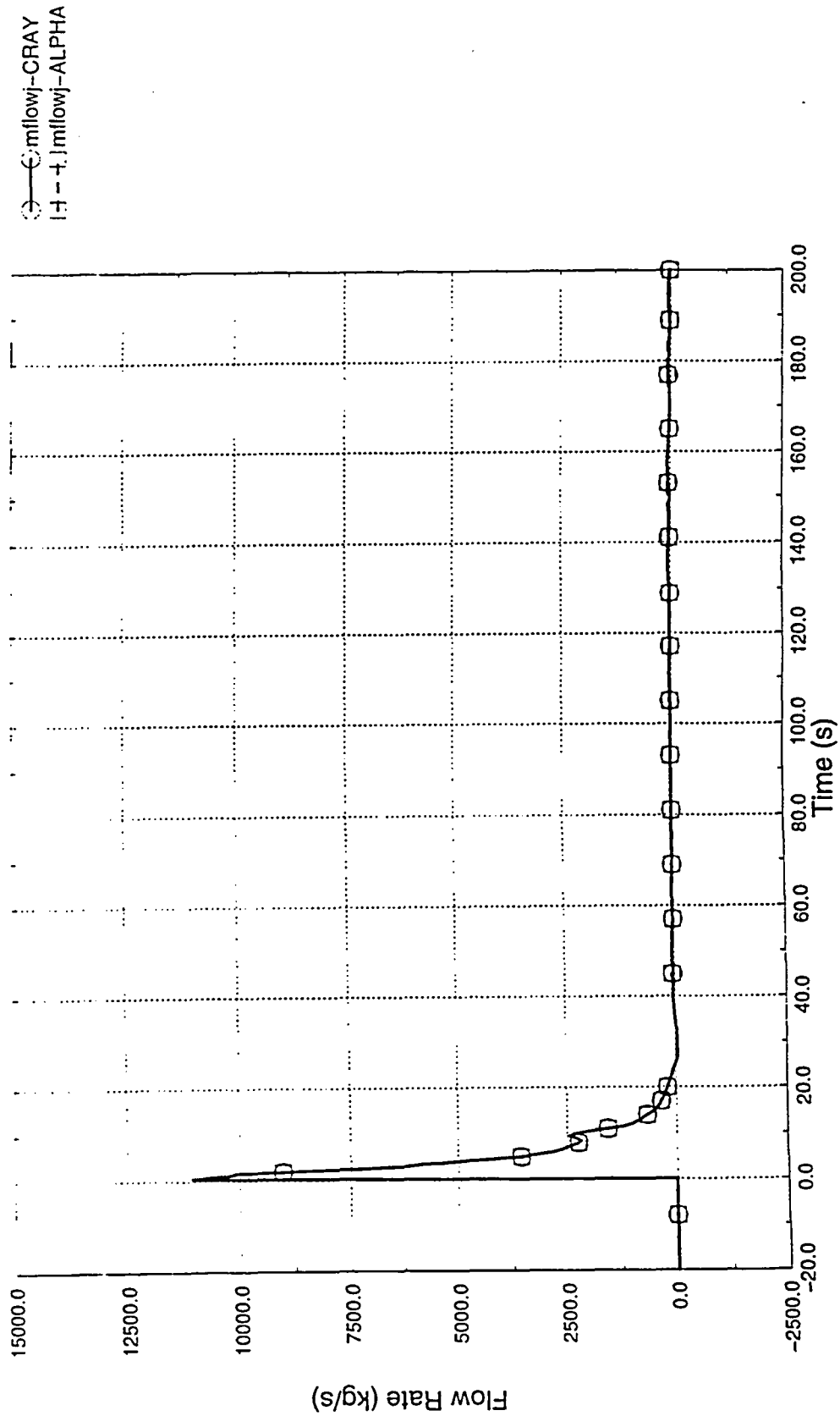

Figure 4 Integrated Mass Flow at Break (pump side)

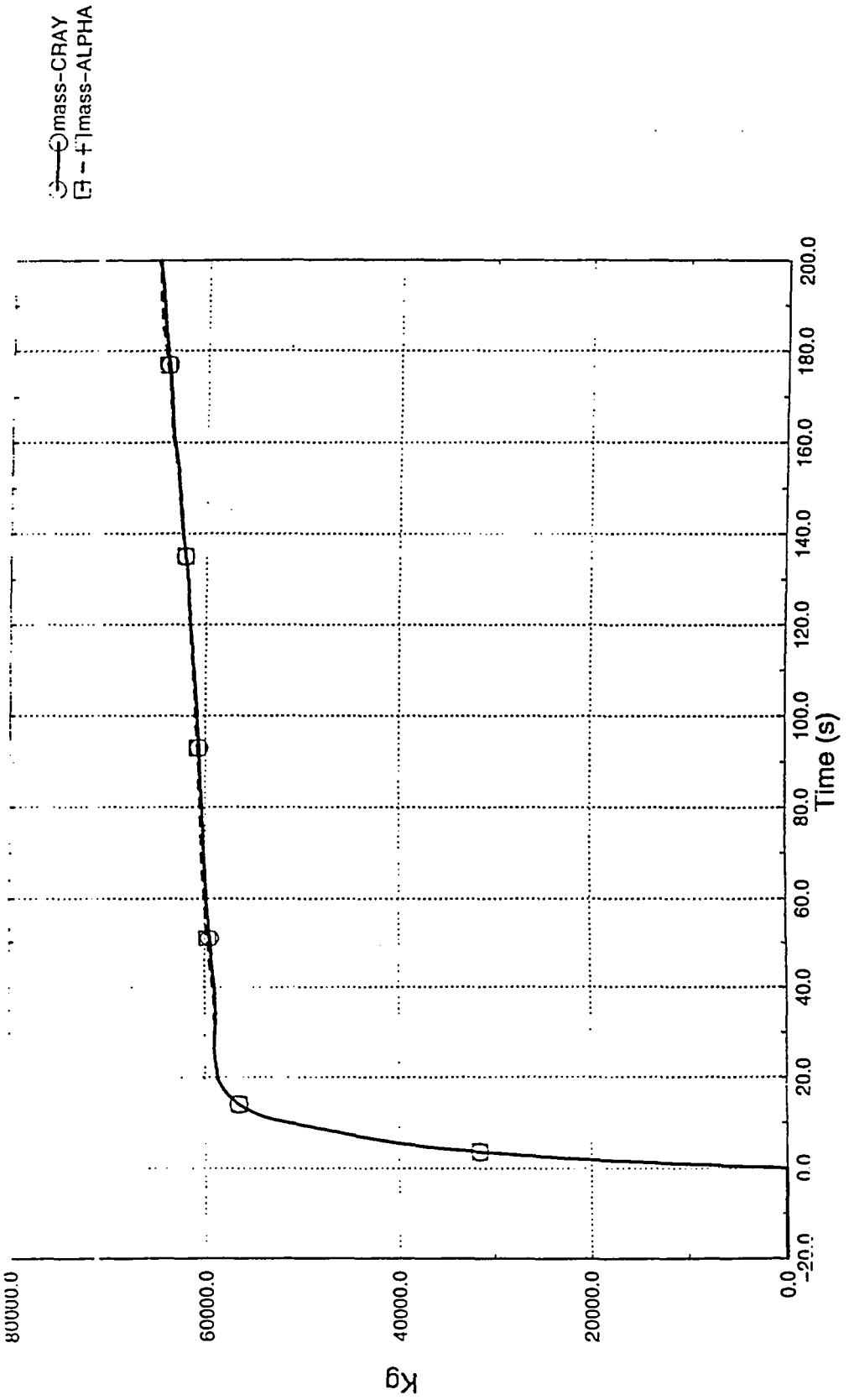

Figure 5. Break Mass Flow (vessel side)

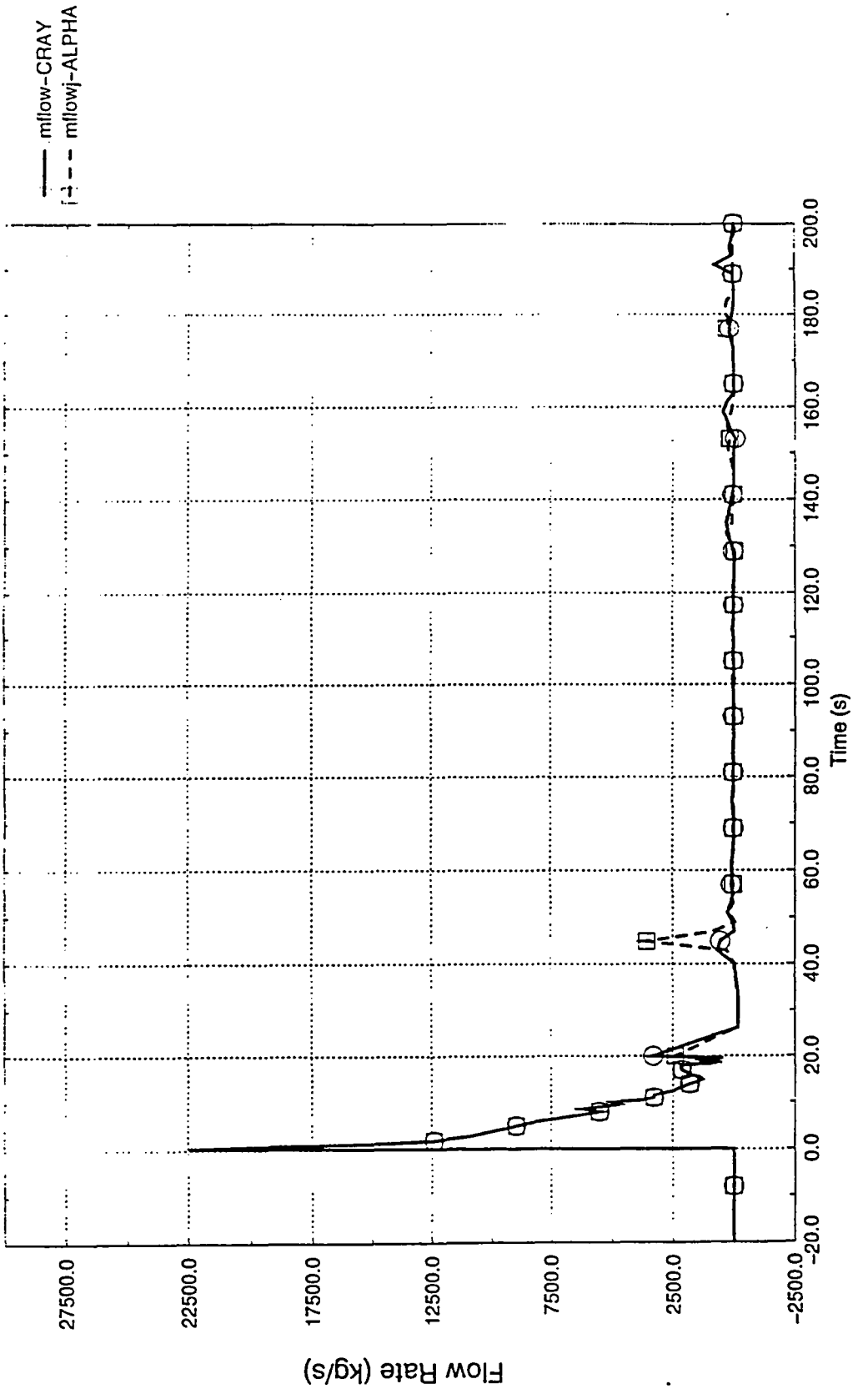

Figure 6. Integrated Mass Flow at Break (vessel side)

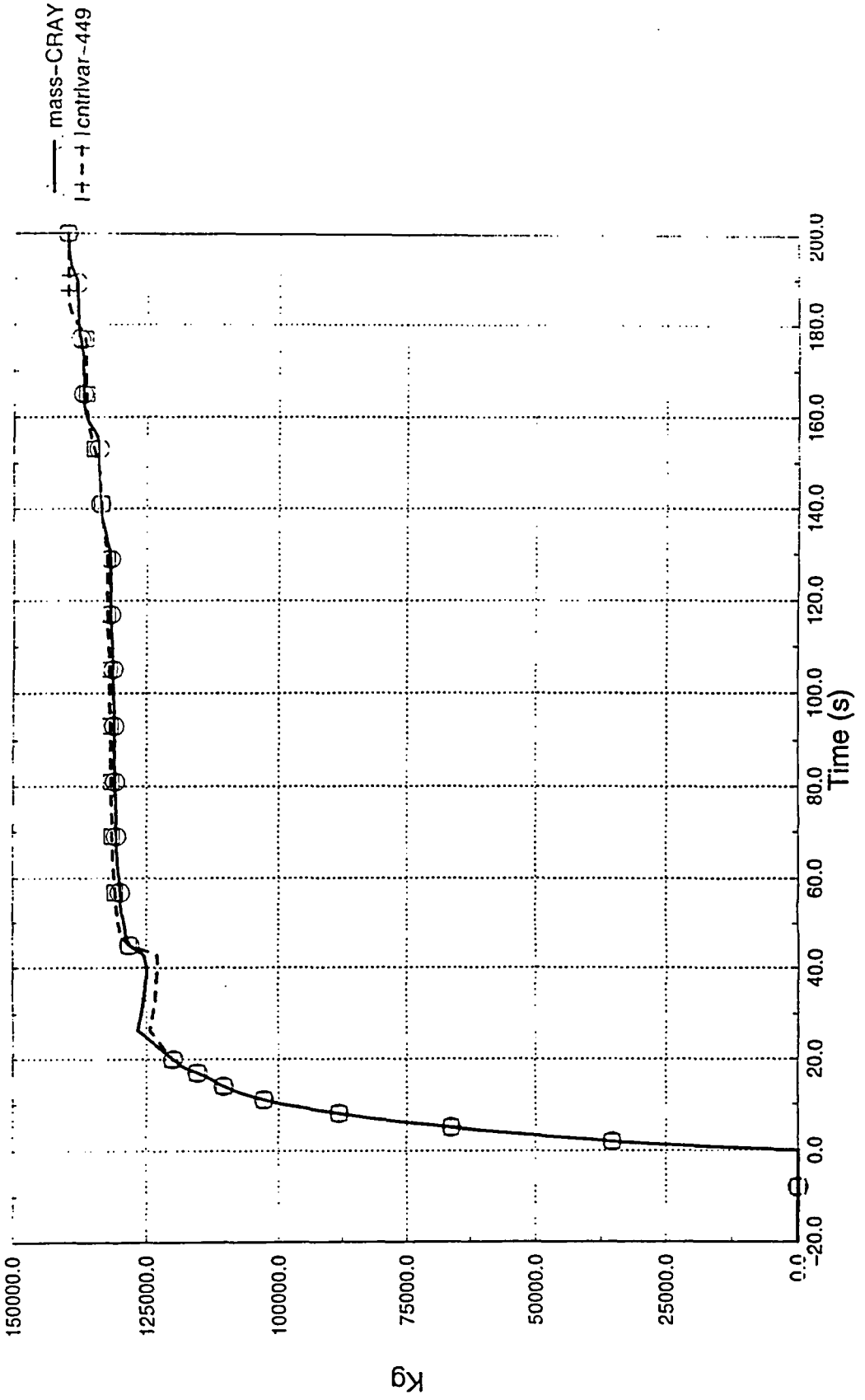

Figure 7. Pressurizer Pressure.

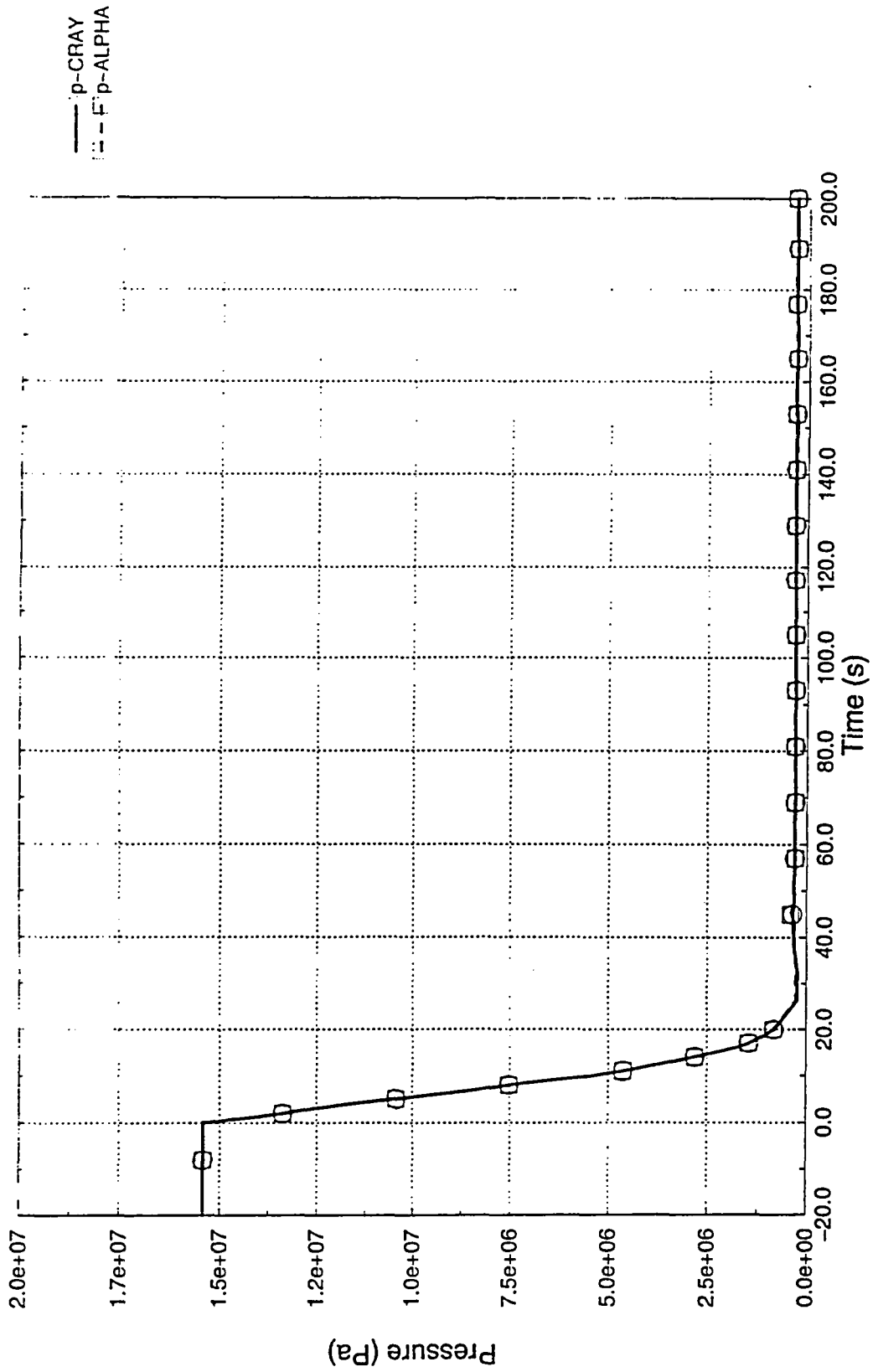

Figure 8. Accumulator Mass Flow (intact loop 1)

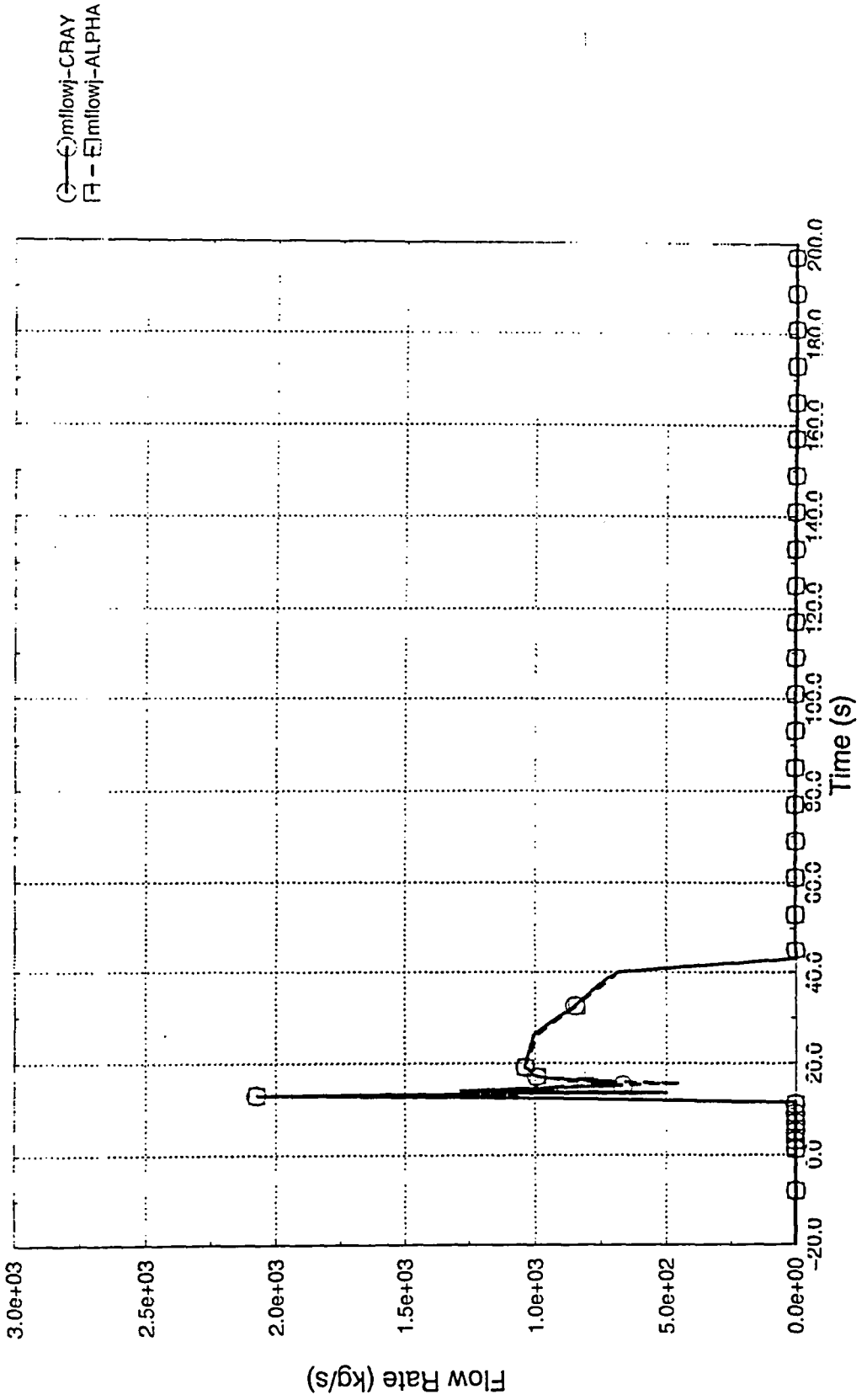

Figure 9. Core Collapsed Liquid Level (hot channel)

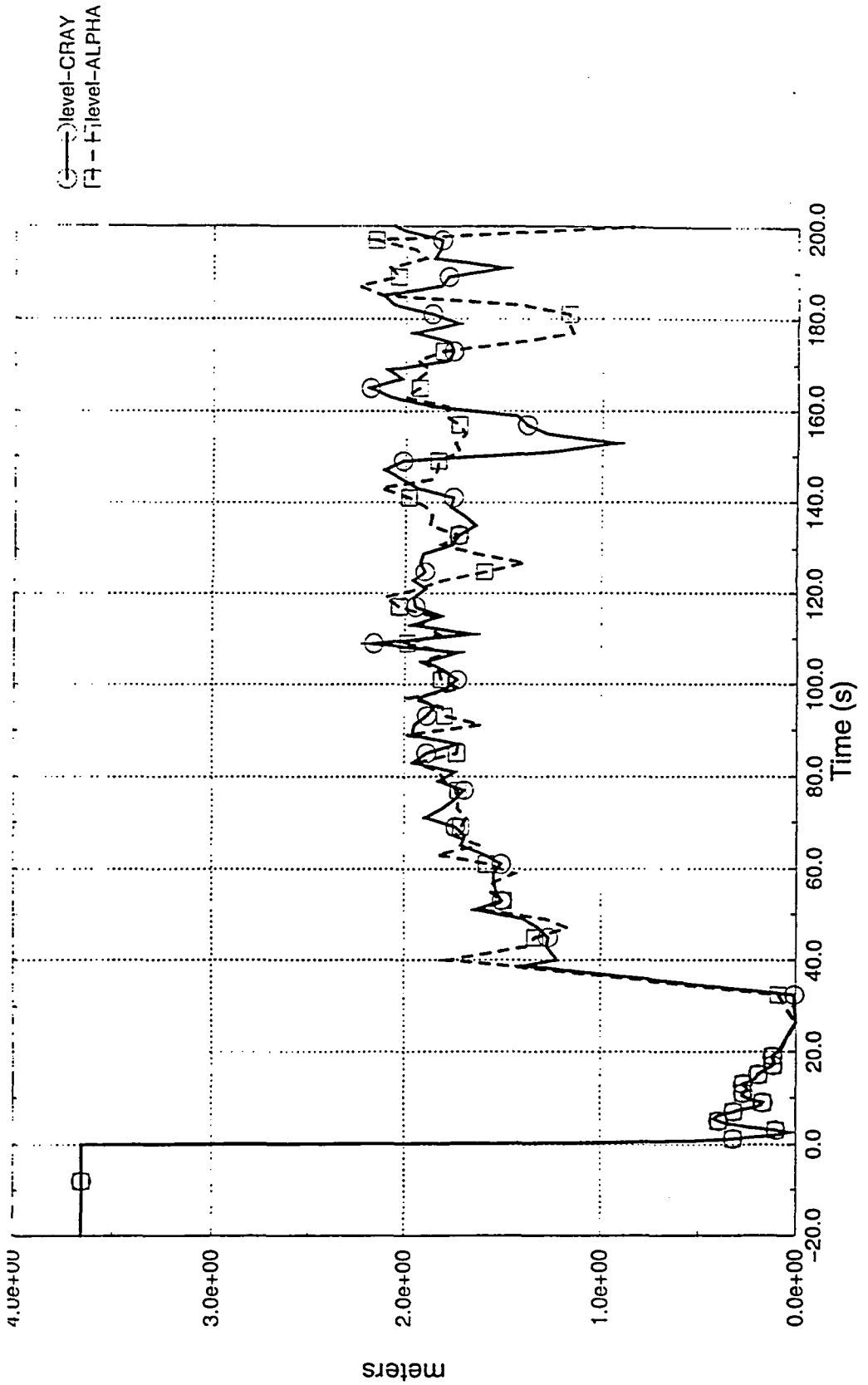

Figure 10. Downcomer Liquid Level

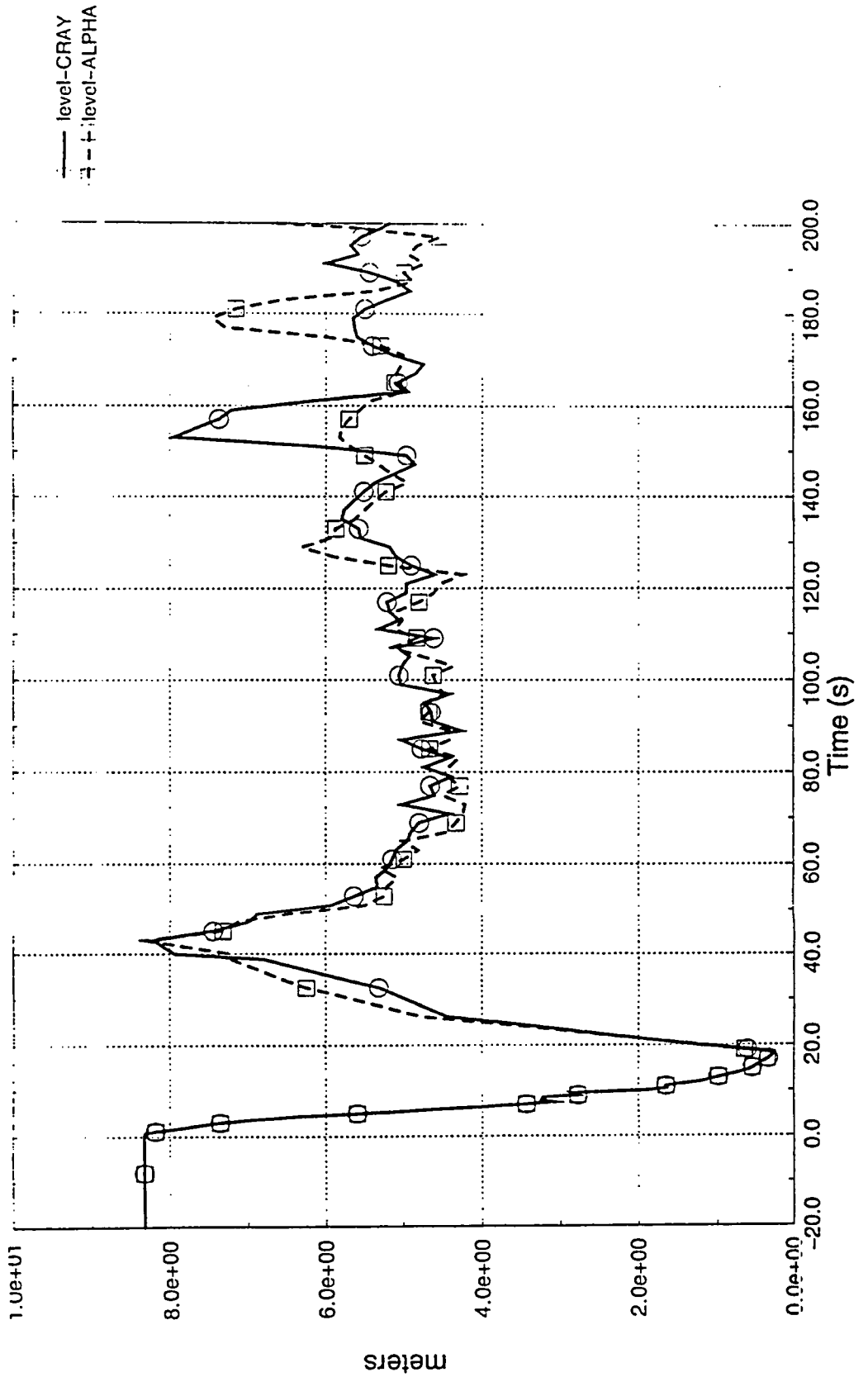

Figure 11. Core Inlet Flow (hot channel)

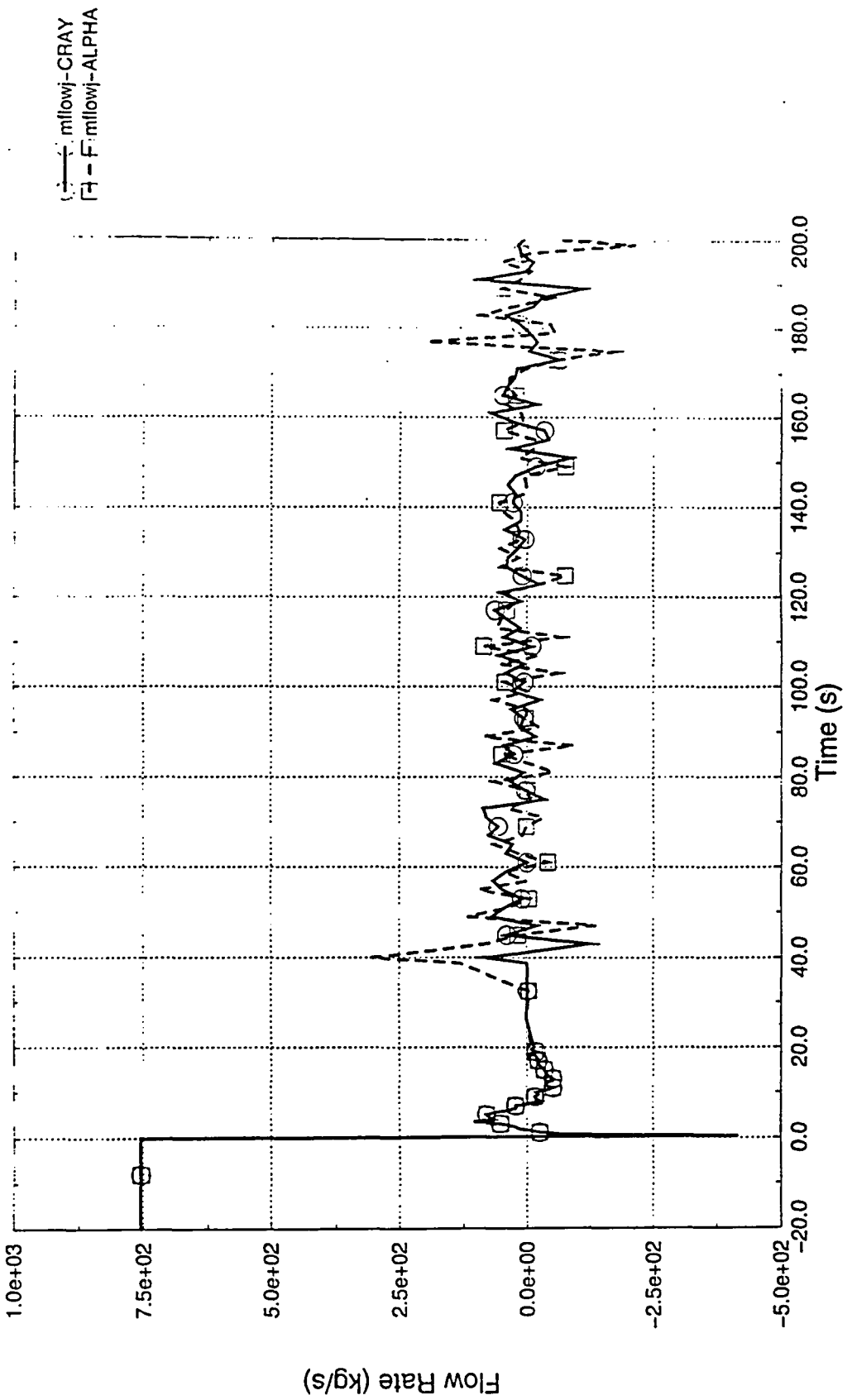

Figure 12. Core Outlet Flow (hot channel).

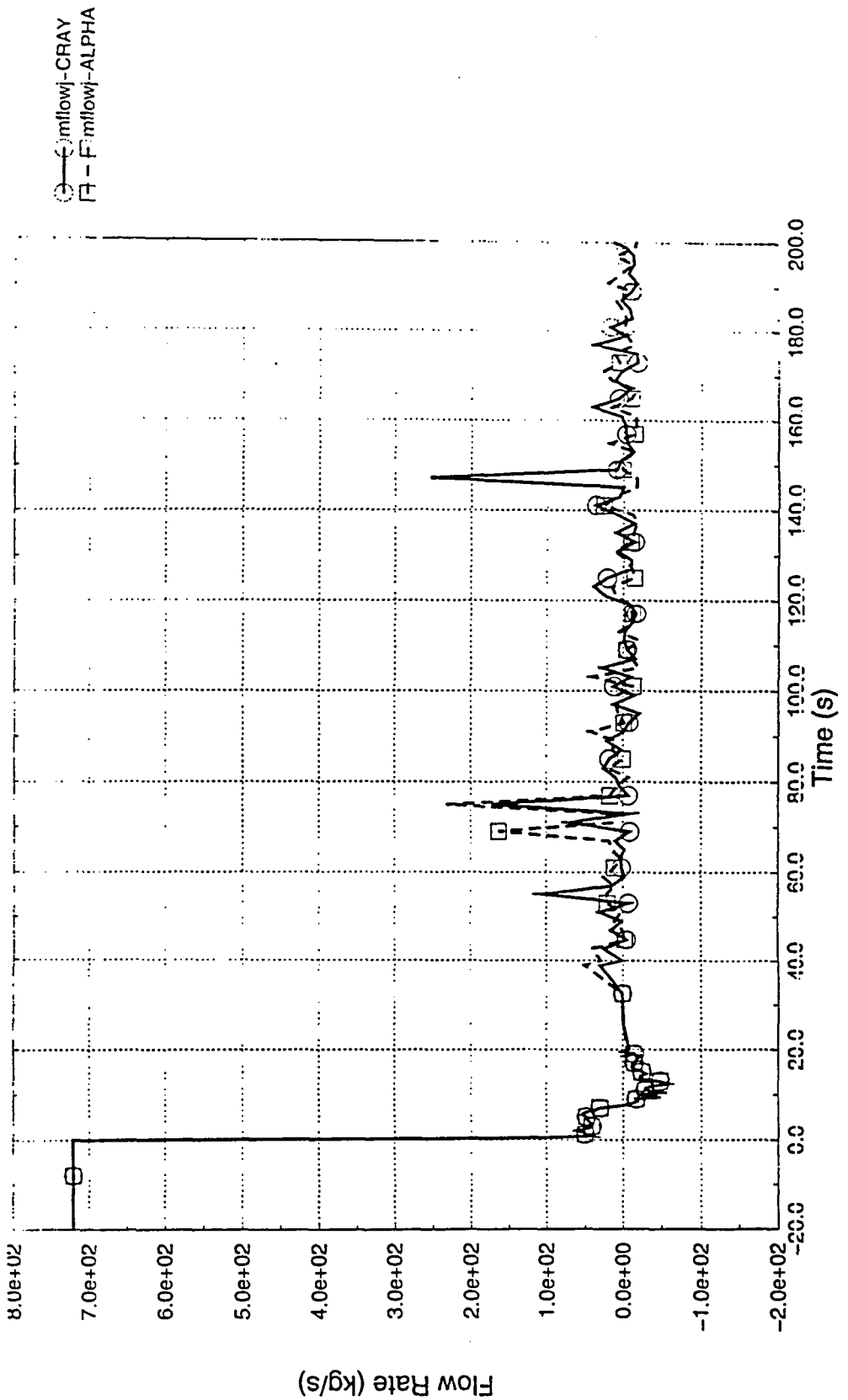

Figure 13. Clad Temperature at Pos. 7.

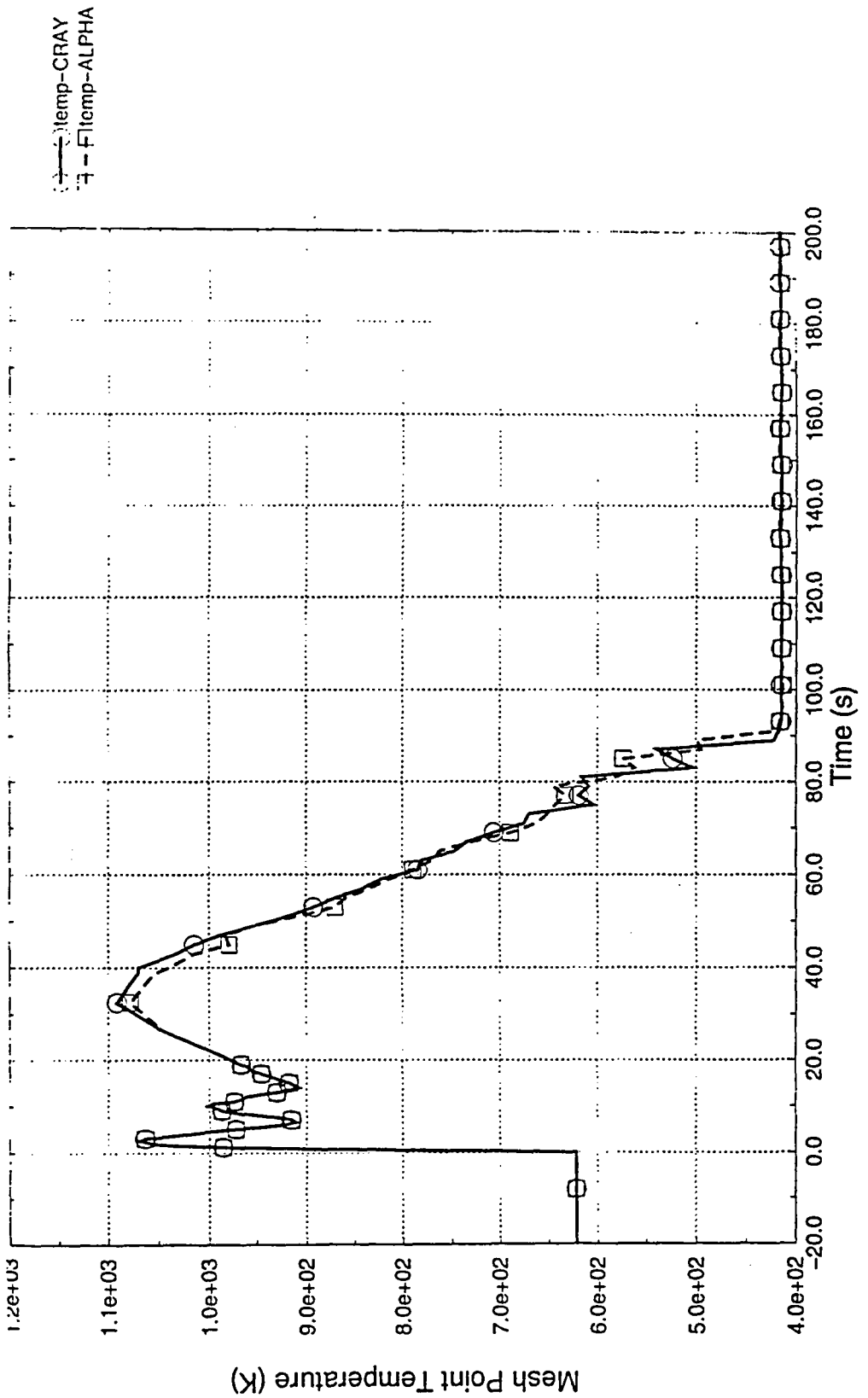

Figure 14. Clad Temperature at Pos. 8

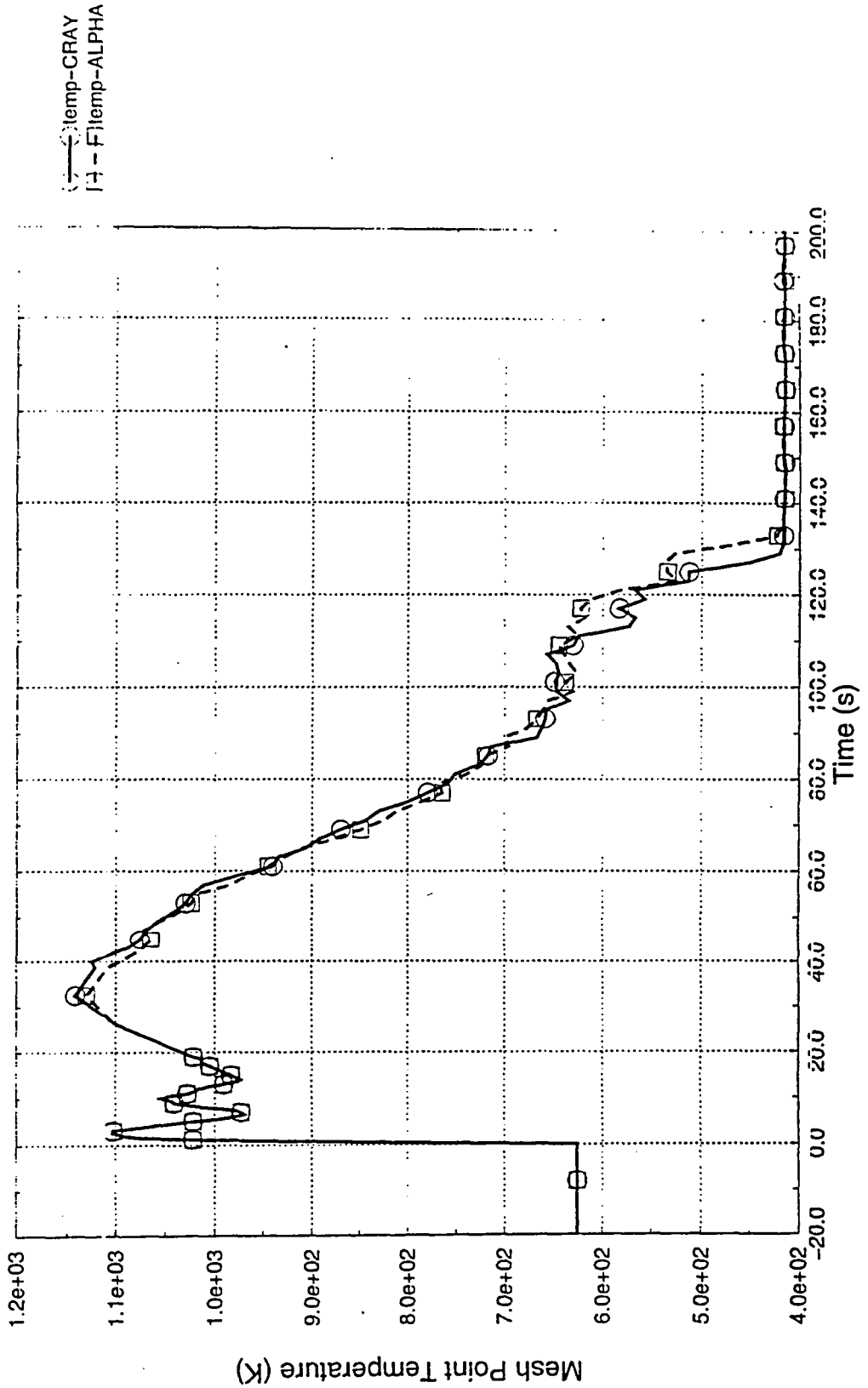

Figure 15. Clad Temperature at Pos. 9

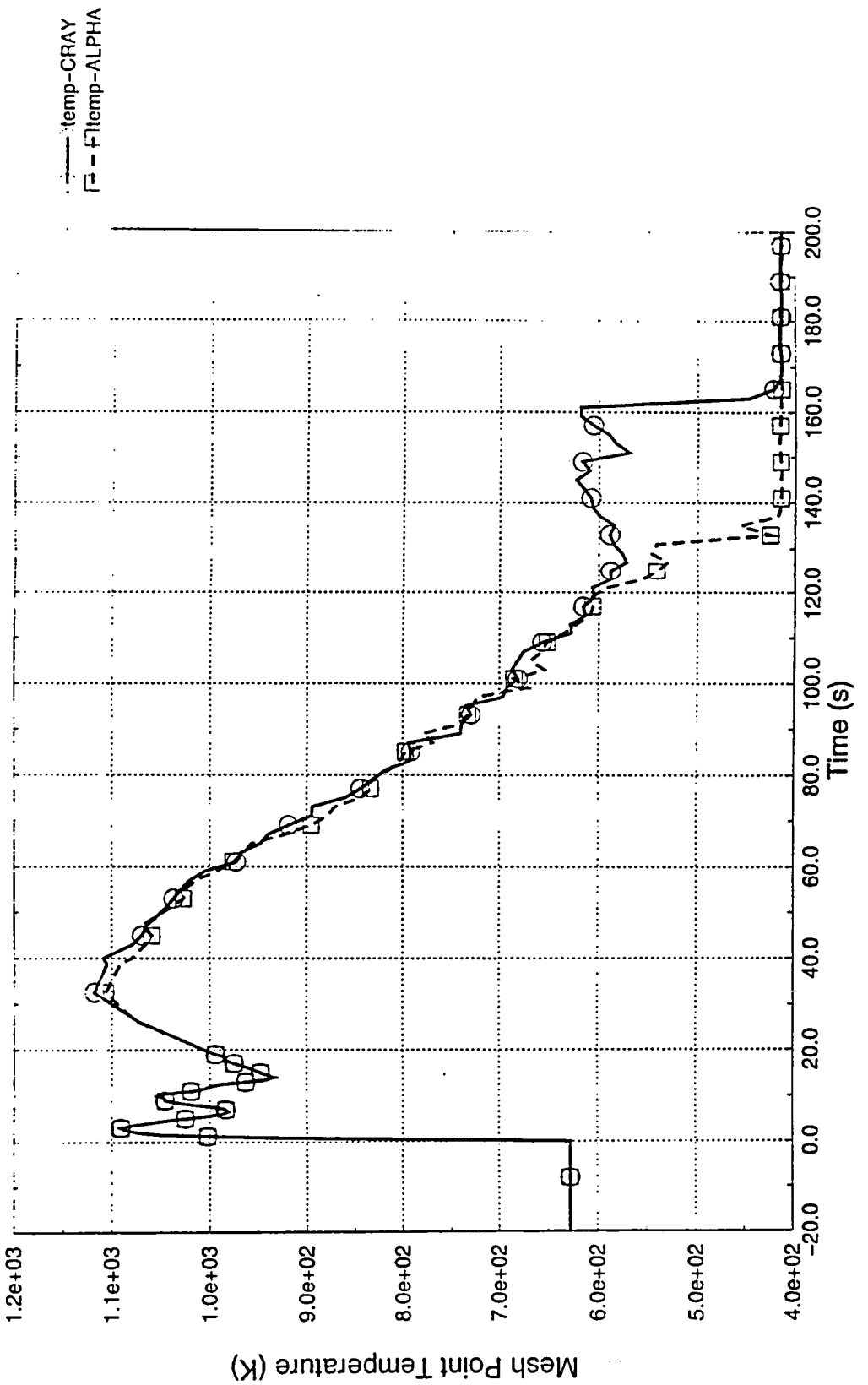

Figure 16. Clad Temperature at Pos. 10

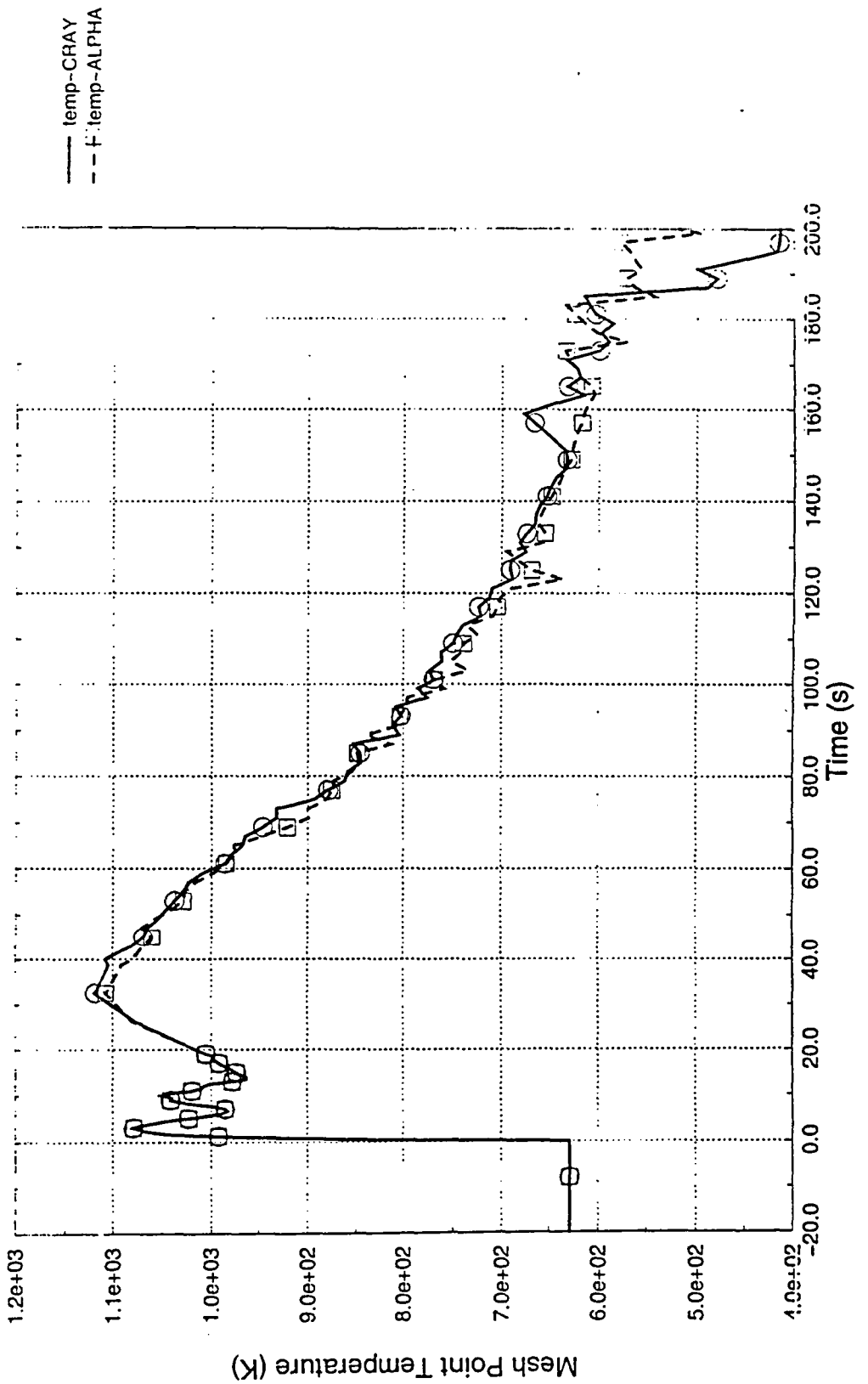

Figure 17. Clad Temperature at Pos. 11

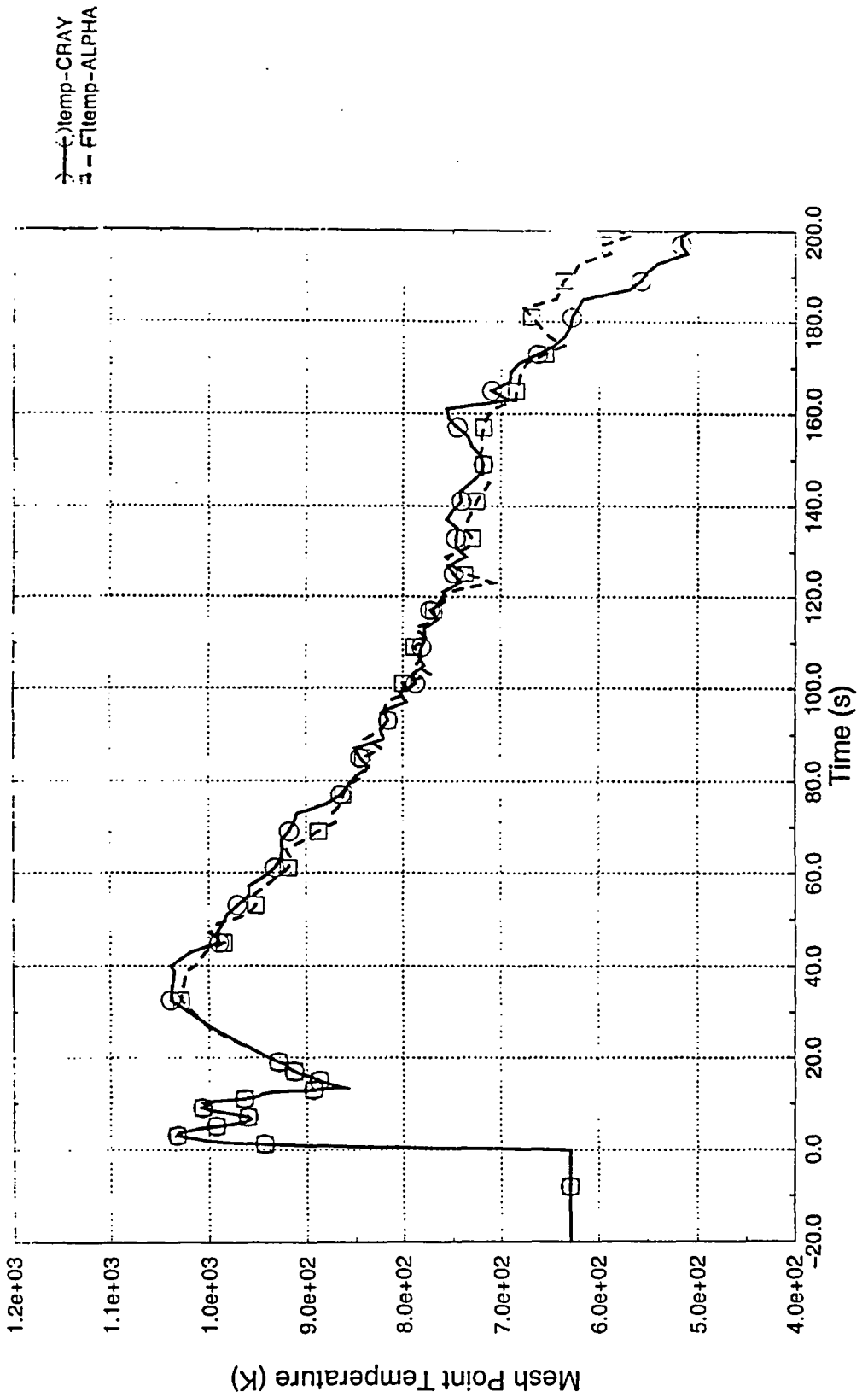

Figure 18. Clad Temperature at Pos. 12

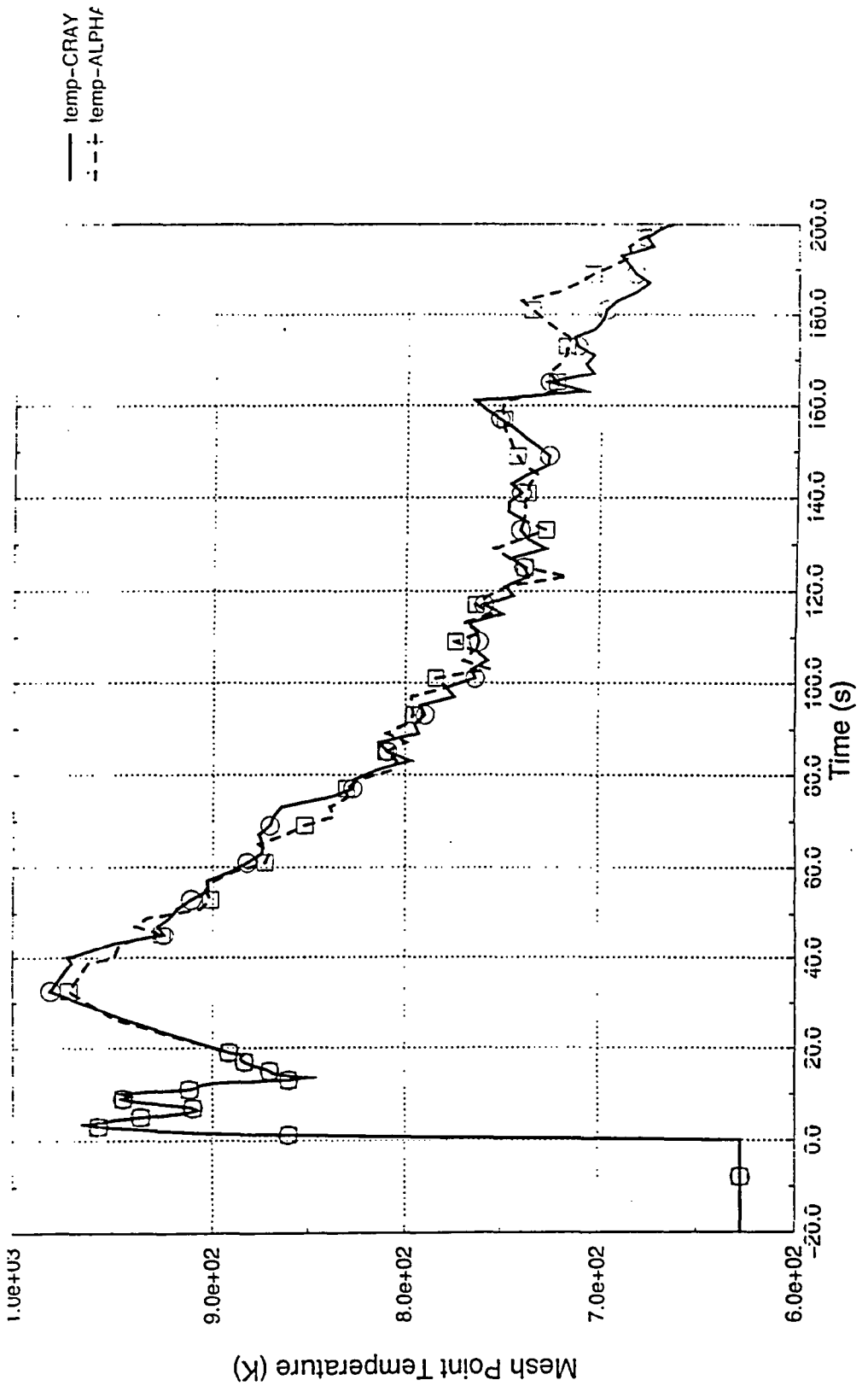

Figure 19. CPU Time

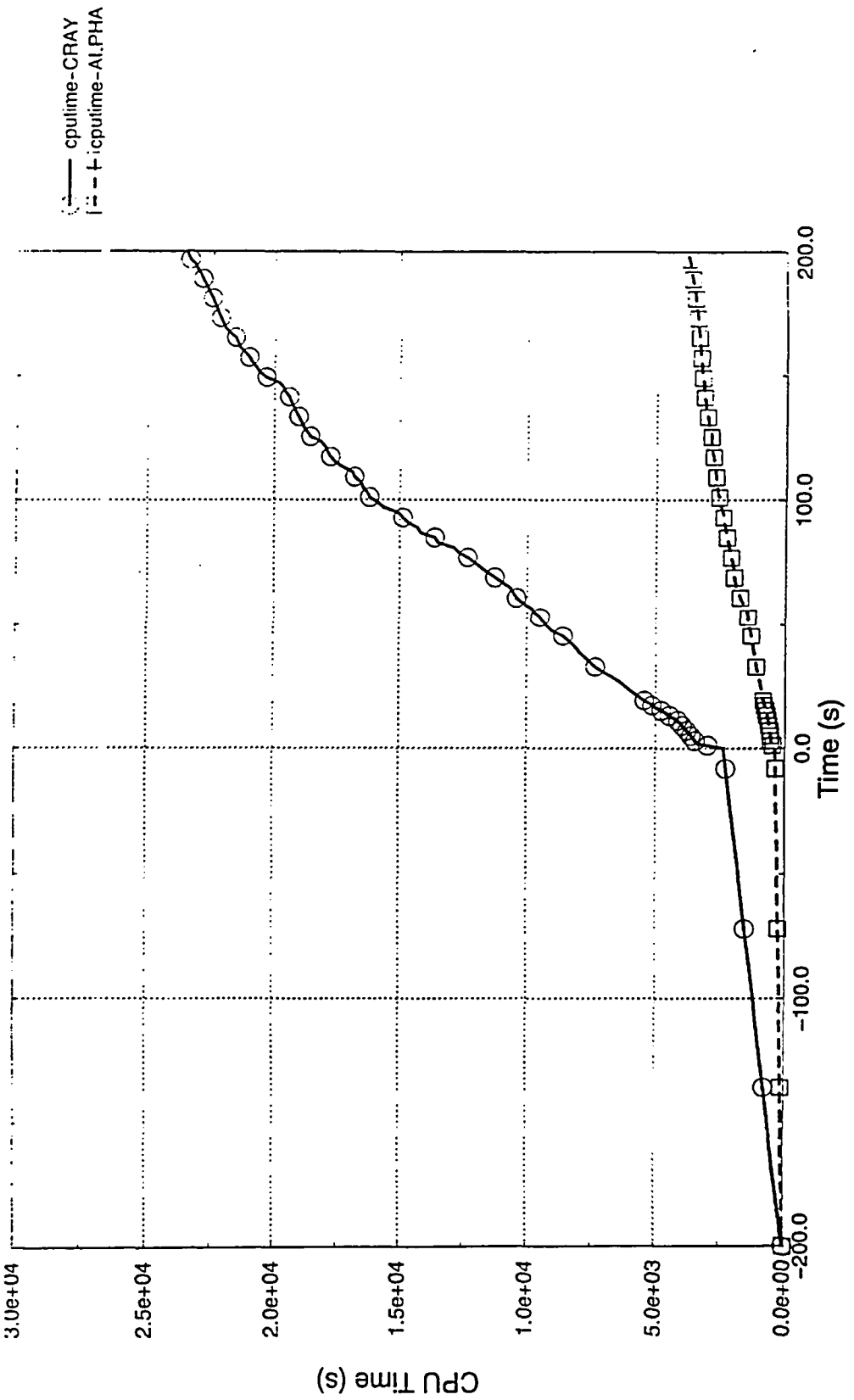

5. CASE 2: RESULTS OBTAINED BY MODELING A COLLAPSED AND A PSEUDO THREE-DIMENSIONAL DOWNCOMER.

Traditionally, one of the most important limitations for using RELAP5/MOD2 in the LBLOCA analysis has been the lack of a three-dimensional component to model the three- dimensional effects that are anticipated to occur in the Reactor Pressure Vassel and, in particular, in the downcomer.

The use of cross flow components allows the user to model three-dimensional geometries, but the momentum flux terms are neglected in these cross flow junctions. In practice, the use of cross flow junctions has been limited to leak flow paths with low flows compared with the main stream.

Several improvements to the cross flow model have been made since the release of RELAP5/MOD2. The latest version, RELAP5/MOD3.2, includes an improved cross flow model. Momentum in the cross flow junctions is conserved, but it's not a full three-dimensional model, because transport of the momentum between one direction and another is not modelled.

Taking into consideration these limitations, a new nodalization was made that only differs in the modelling of the downcomer. In the first run, the nodalization models the downcomer as a single pipe of 8 cells (previous nodalization used in Case 1). In the second run, the downcomer is modelled as made up of three pipes (of 8 cells) joined by cross flow junctions. The results of this second run with the three-dimensional downcomer was then compared with the first run to check the effect of the downcomer nodalization on the ECCS bypass flow and the lower plenum swept out.

Fig. 20 shows the pressurizer pressure for both runs.

Figs. 21 and 22 show the integrated mass flow at the break location on the pump and vessel side, respectively. It can be observed that the integrated mass flow is, on the pump side, very close in both cases. Nevertheless, on the vessel side of the break, the mass flow delivered differs for both cases, with the break mass flow rate for the collapsed nodalization model being higher than when the three-dimensional nodalization is used.

Looking at Fig. 22, it would be expected that the three-dimensional nodalization model would predict more liquid in the vessel. This can be seen in Fig. 23 which plots the liquid fraction in the lower plenum. In the three dimensional nodalization, the lower plenum is refilled earlier than in the collapsed nodalization model. The ECCS bypass flow is higher in the collapsed nodalization model, than in the three dimensional nodalization. Fig. 24 shows the core inlet mass flow in the hot channel. The liquid enters the core earlier in the three-dimensional nodalization. The core liquid level can be observed in Fig. 25 (obtained by multiplying the cell lengths by their liquid void fractions).

Figures 26 through 31 show the cladding temperatures obtained at different elevations (the core was modelled with 15 axial elevations). Due to the higher amount of liquid calculated with the three-dimensional nodalization, the cladding temperatures are clearly lower than for the collapsed nodalization downcomer model. Finally, Fig. 32 shows the collapsed downcomer level (obtained by multiplying the cell lengths by their

liquid void fractions) in the three downcomer pipes used to model the three-dimensional downcomer. The labels *"broken"*, *"intact1"* and *"intact2"* are used to indicate to which of the downcomer pipe components, the broken cold leg is joined to. It can be observed that the amount of liquid in the downcomer pipe connected to the broken cold leg is lower during the blowdown, and slightly higher than in the rest of the downcomer pipes due to the sweep phenomena to the break. During refill (approximately 20 sec. after the beginning of the transient), once terminated the ECCS bypass, the liquid in the two downcomer pipes connected to the two intact cold legs are higher due to the ECCS addition, showing the non-symmetric behaviour expected.

The sequence of events and the analysis results are given in Tables 4 and 5. Local oxidation and the burst variables have not been calculated because the gap conductance model and the oxidation model were not used for this second case.

Table 4. Sequence of Events (Case 2).

	Collap. Downcomer run	3D downcomer run
Reactor trip signal	2.0 sec.	2.0 sec.
SI signal generated	3.0 sec.	3.0 sec.
Accumulator injection	11 sec.	11 sec.
End of bypass	19 sec.	18 sec
End of blowdown	26 sec.	26 sec.
Safety injection	26 sec.	26 sec.
Beginning of reflood	31 sec.	28 sec.
Accumulator empties	42 sec.	42 sec.

Table 5. Analysis of Results (Case 2)

	Collap. Downcomer run	3D downcomer run
Peak clad temperature	1125 K	1080 K
Time of peak clad temp.	31 sec.	29 sec.
Peak clad temp. elevation	1.9512 m	1.9512 m
Local oxidation	-	-
Hot rod burst time	-	-
Hot rod burst location	-	-

Figure 20. Pressurizer Pressure.

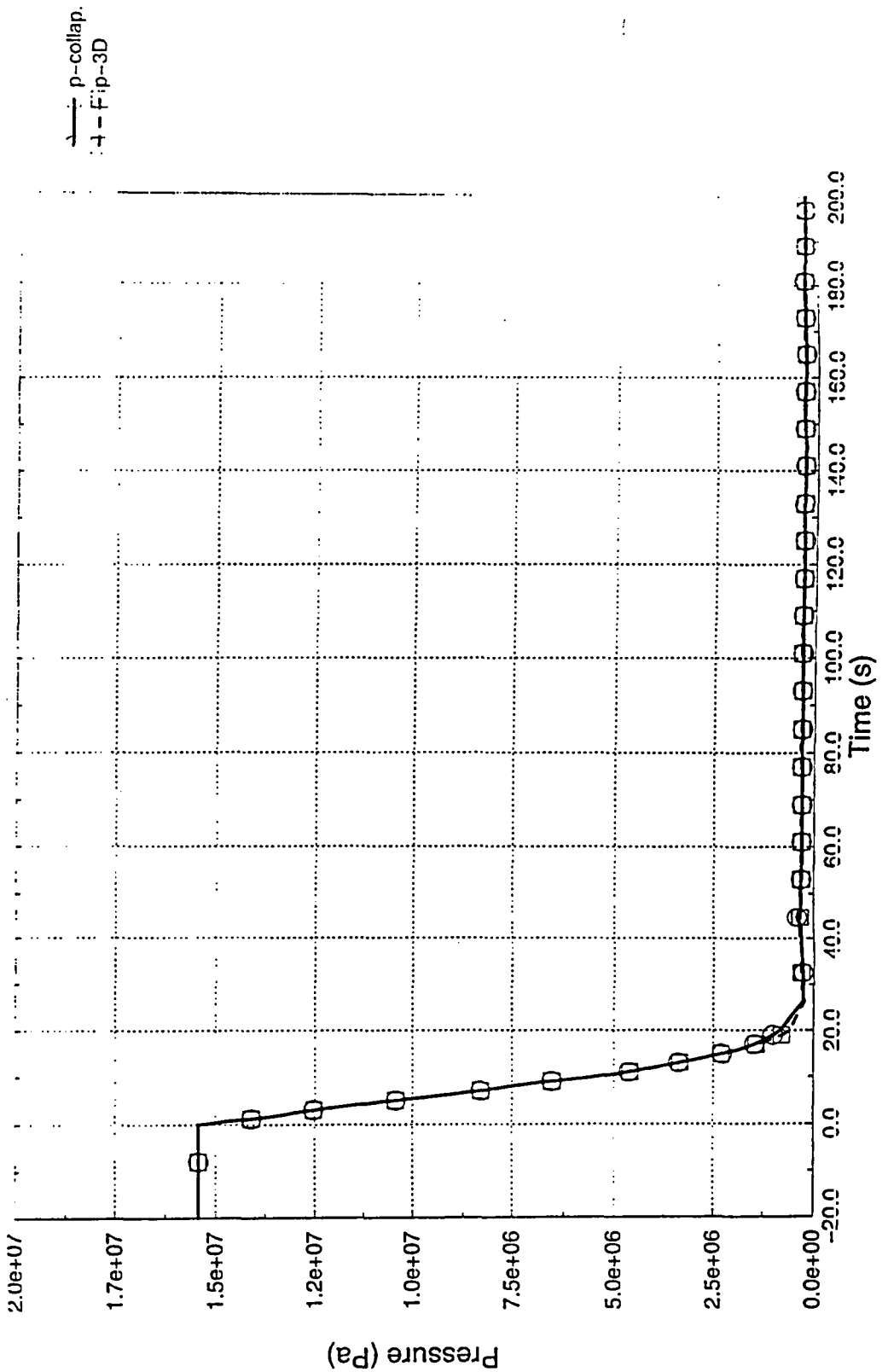

Figure 21. Integrated Mass Flow at Break (pump side)

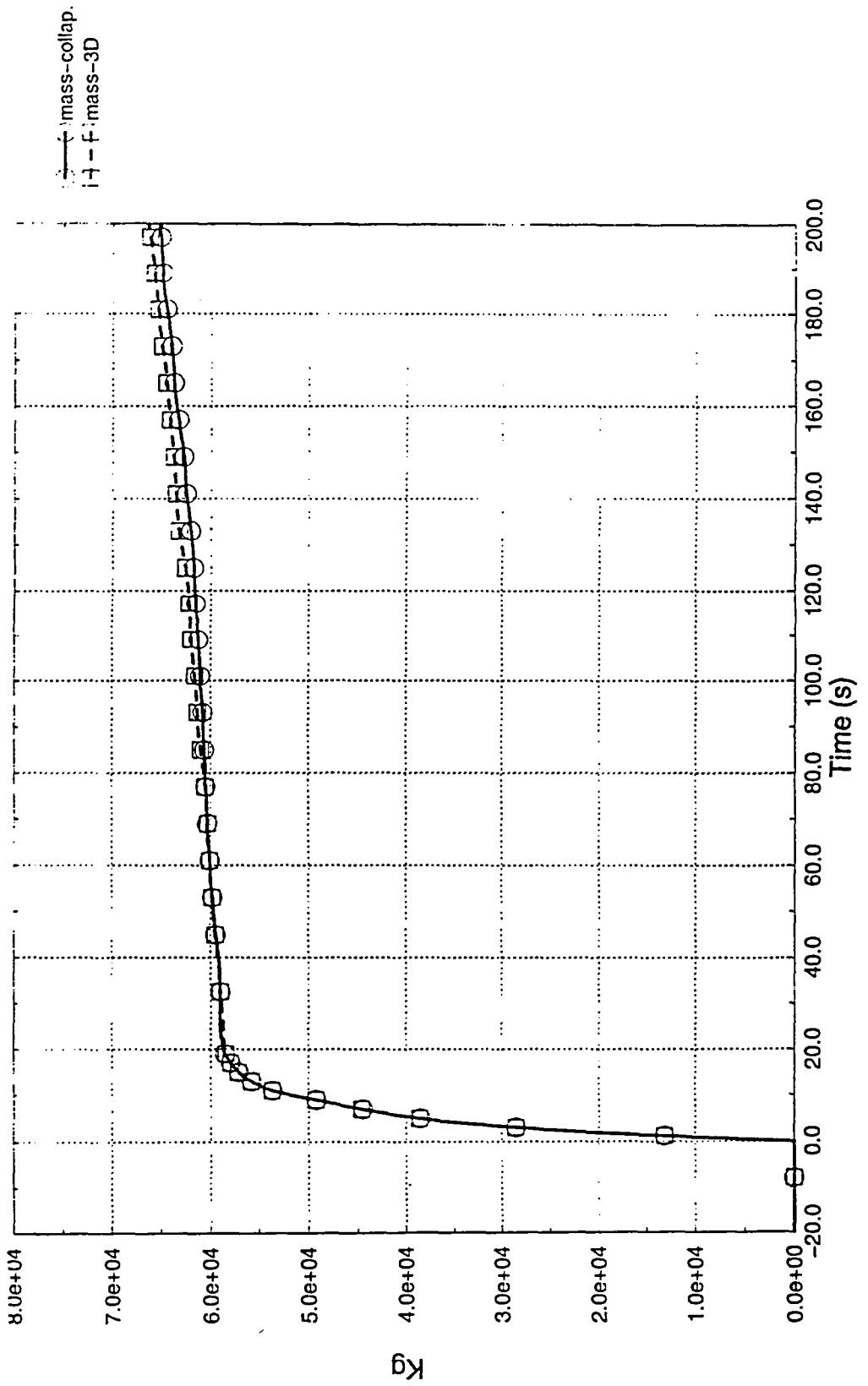

Figure 22. Integrated Mass Flow at Break (vessel side)

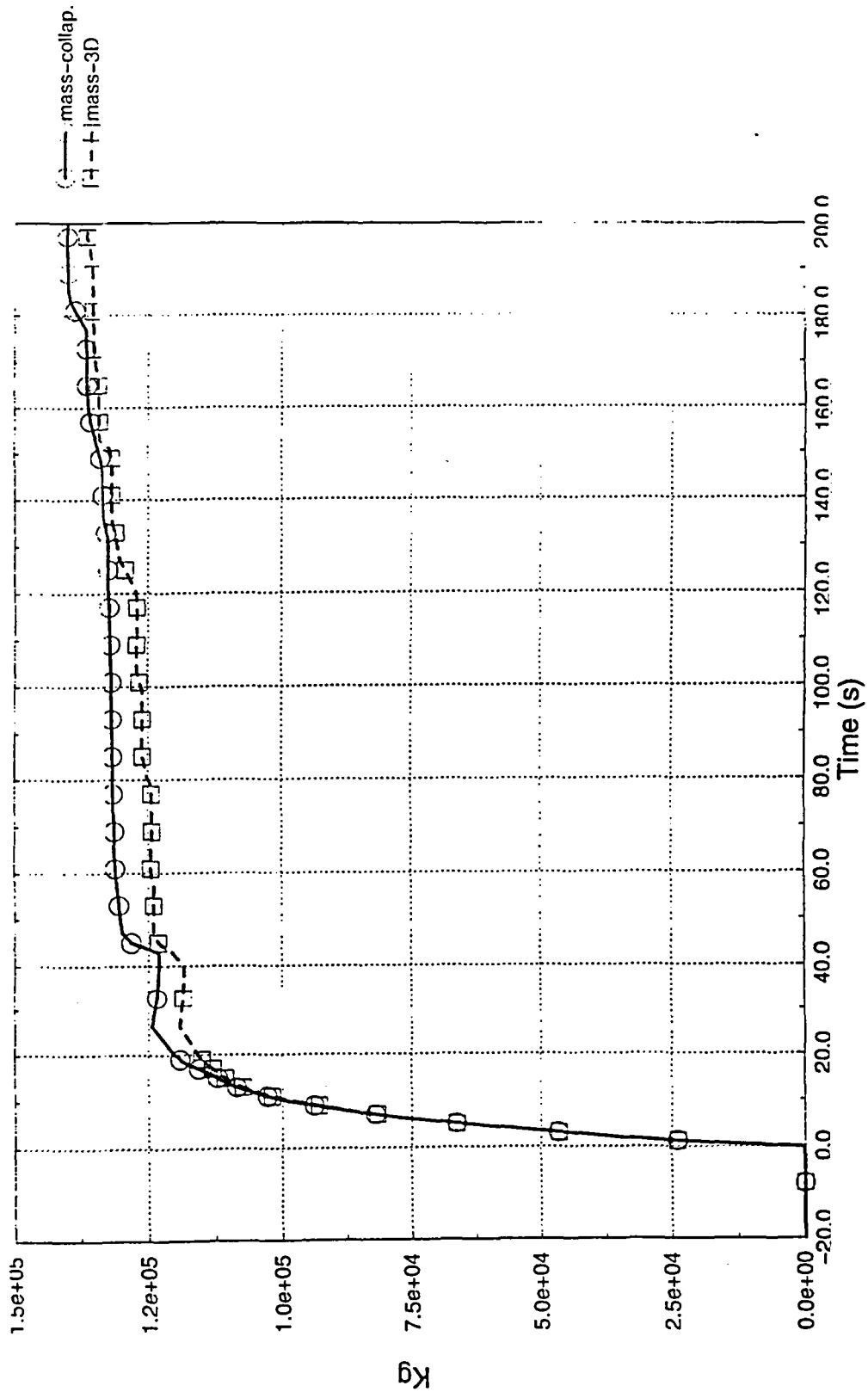

Figure 23. Liquid Fraction in the Vessel Lower Plenum

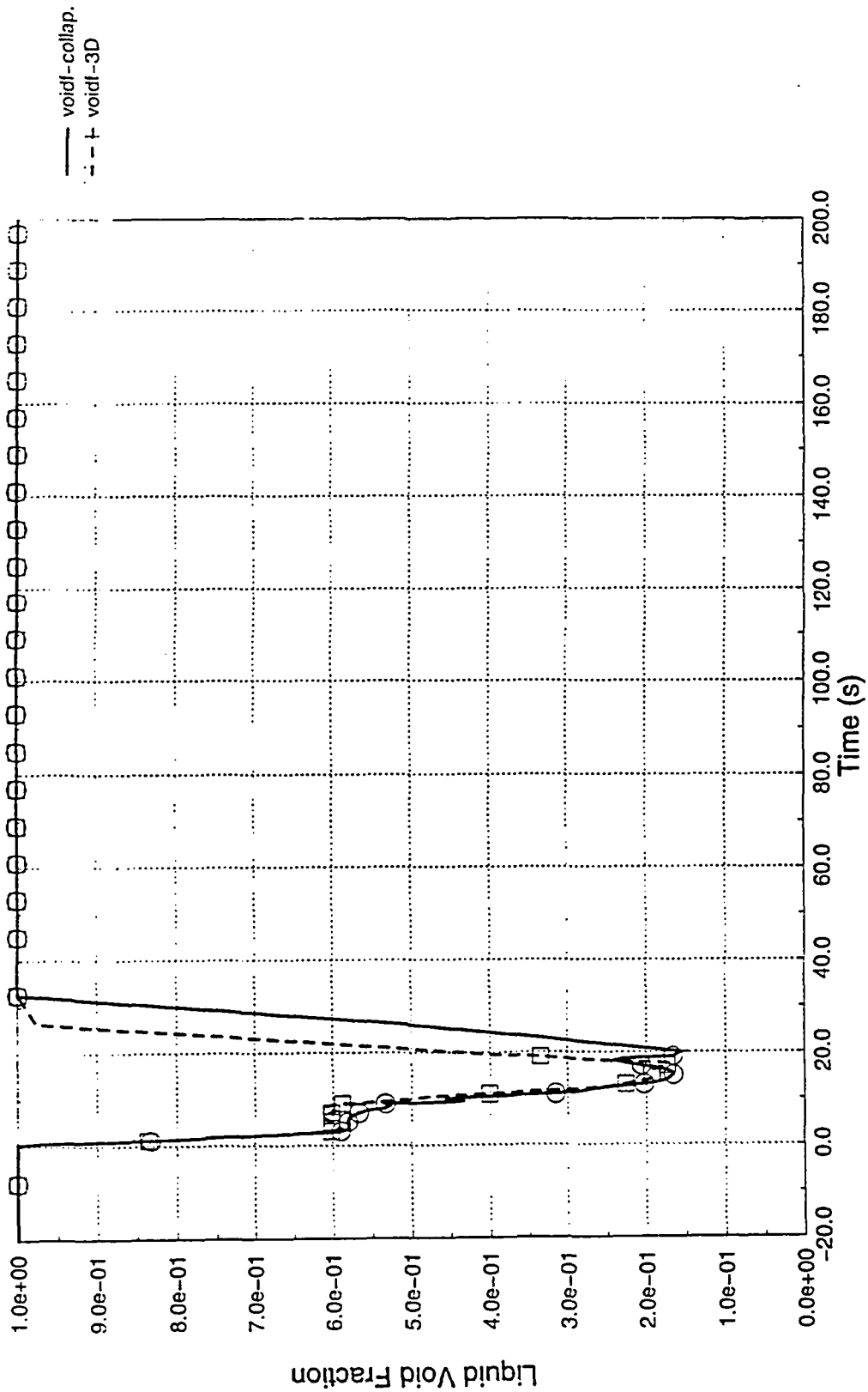

Figure 24. Core Inlet Flow (hot channel)

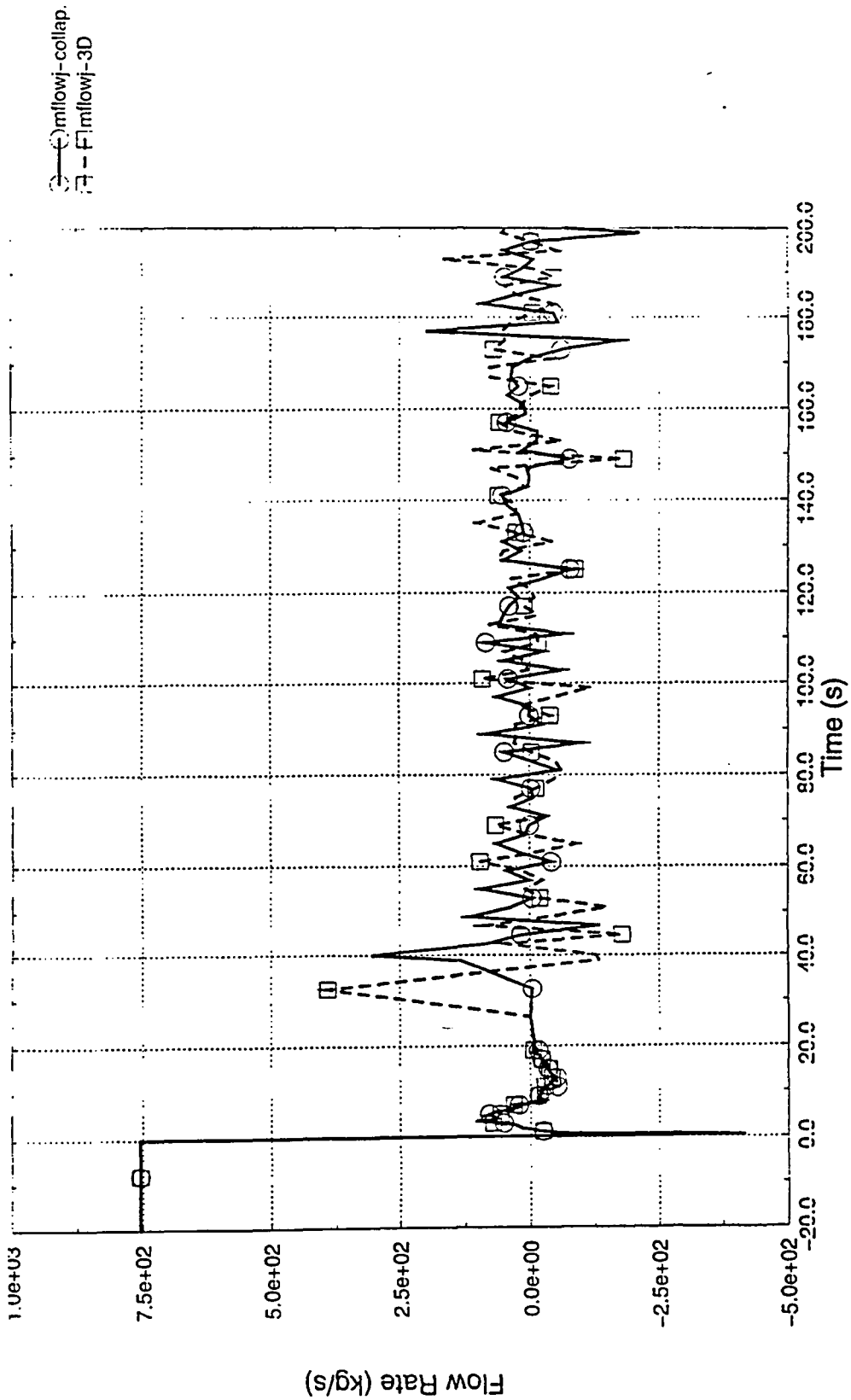

Figure 25. Collapsed Core Liquid Level (hot channel)

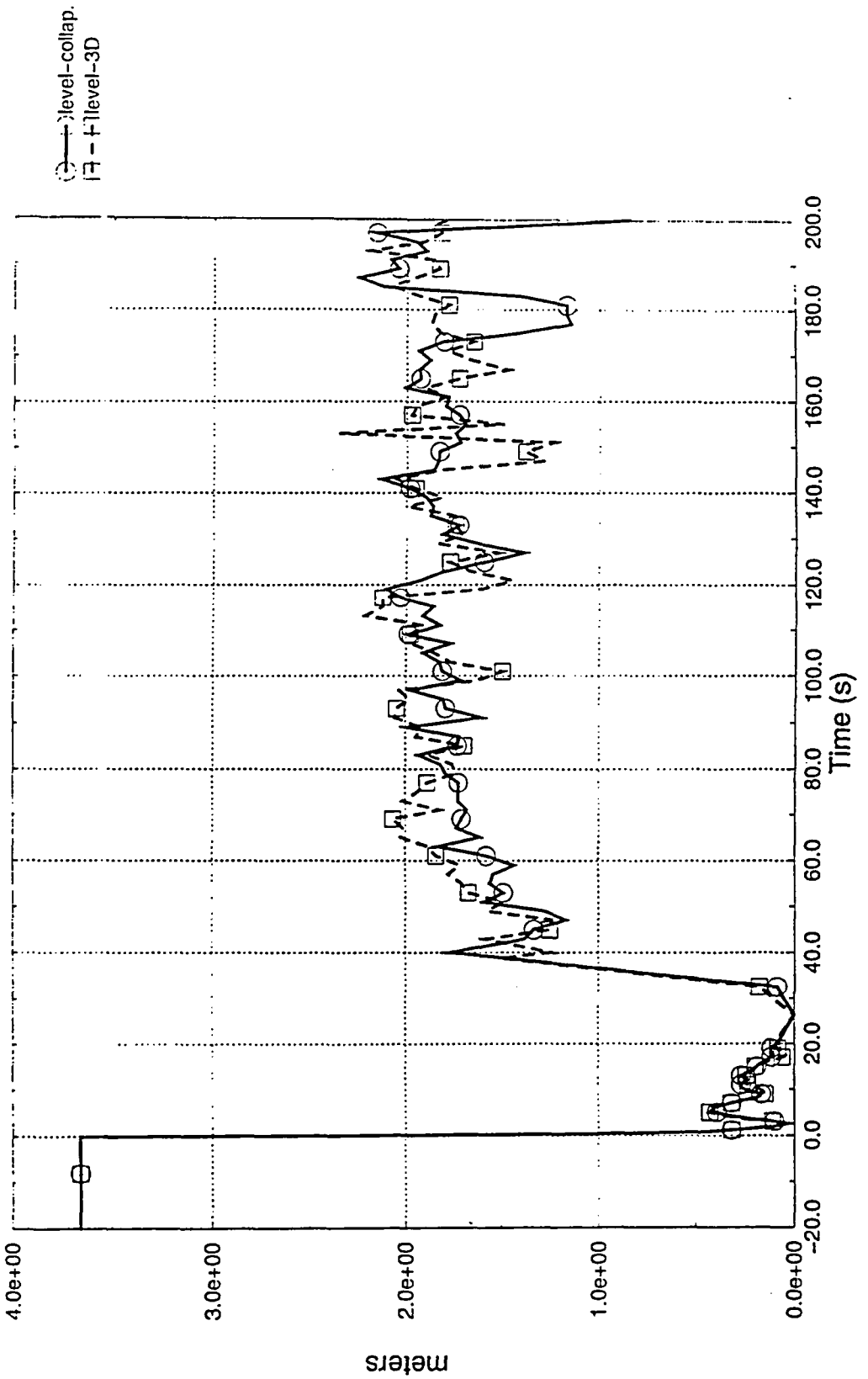

Figure 26. Clad Temperature at Pos. 7 (hot rod)

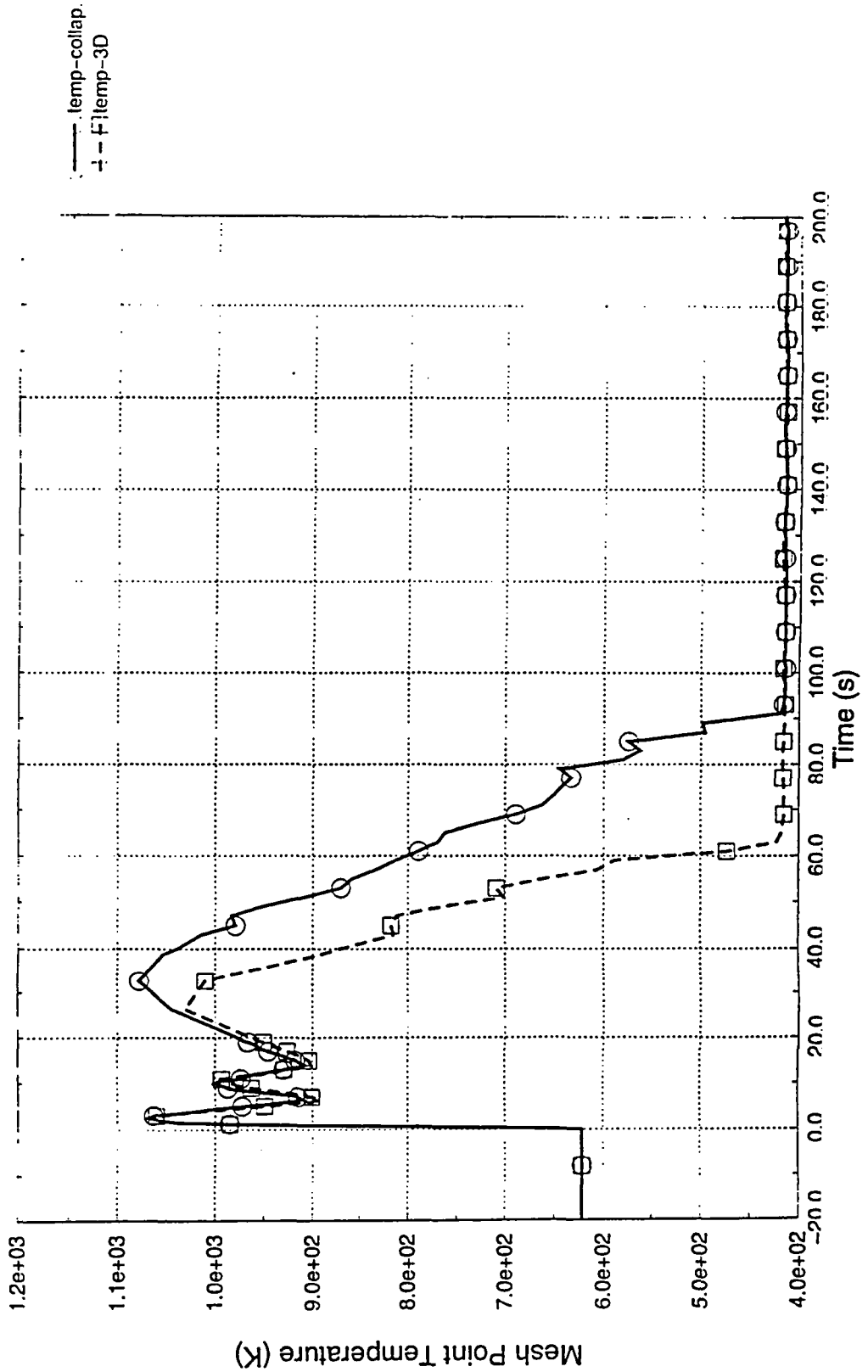

Figure 27. Clad Temperature at Pos. 8 (hot rod)

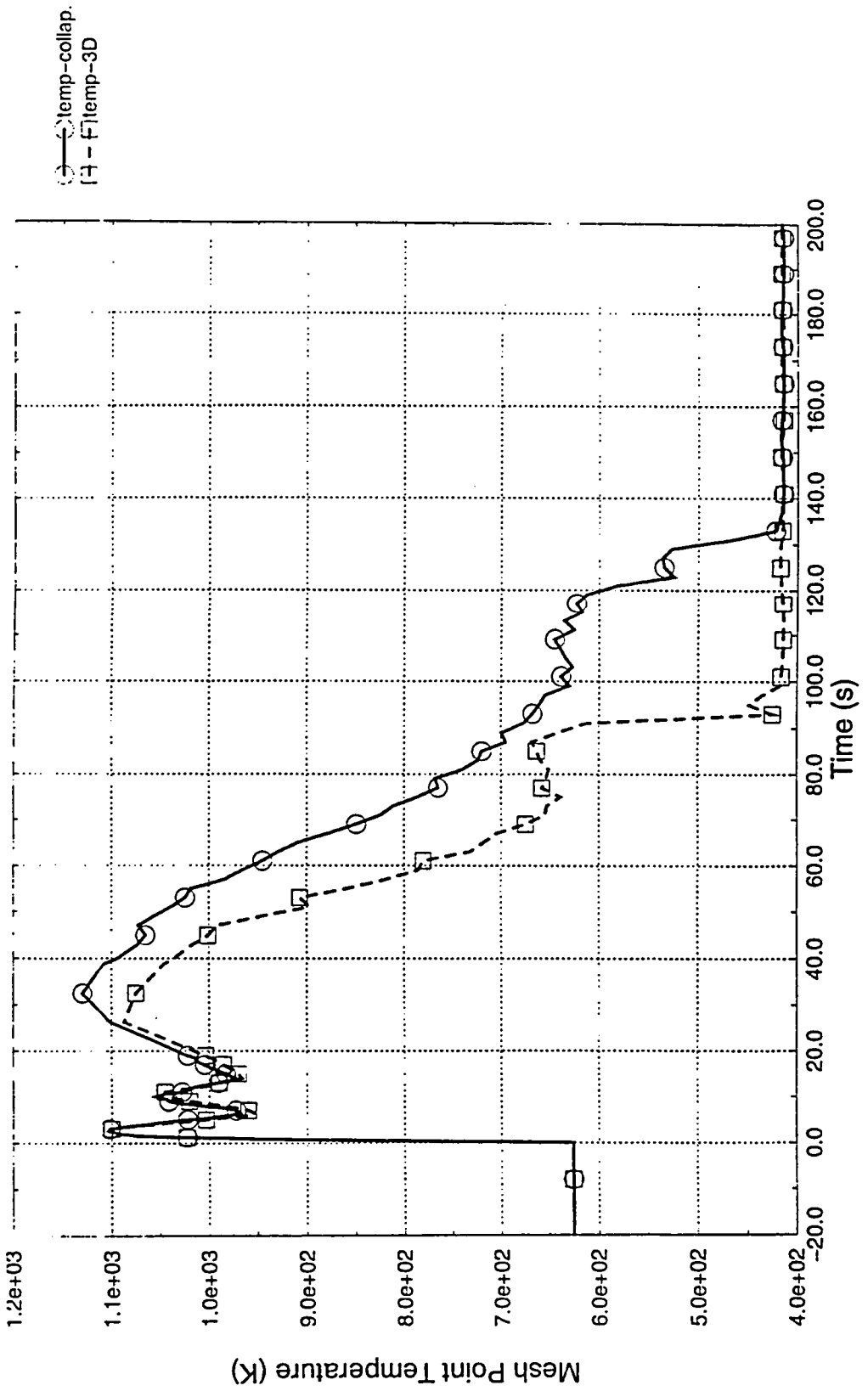

Figure 28. Clad Temperature at Pos. 9 (hot rod)

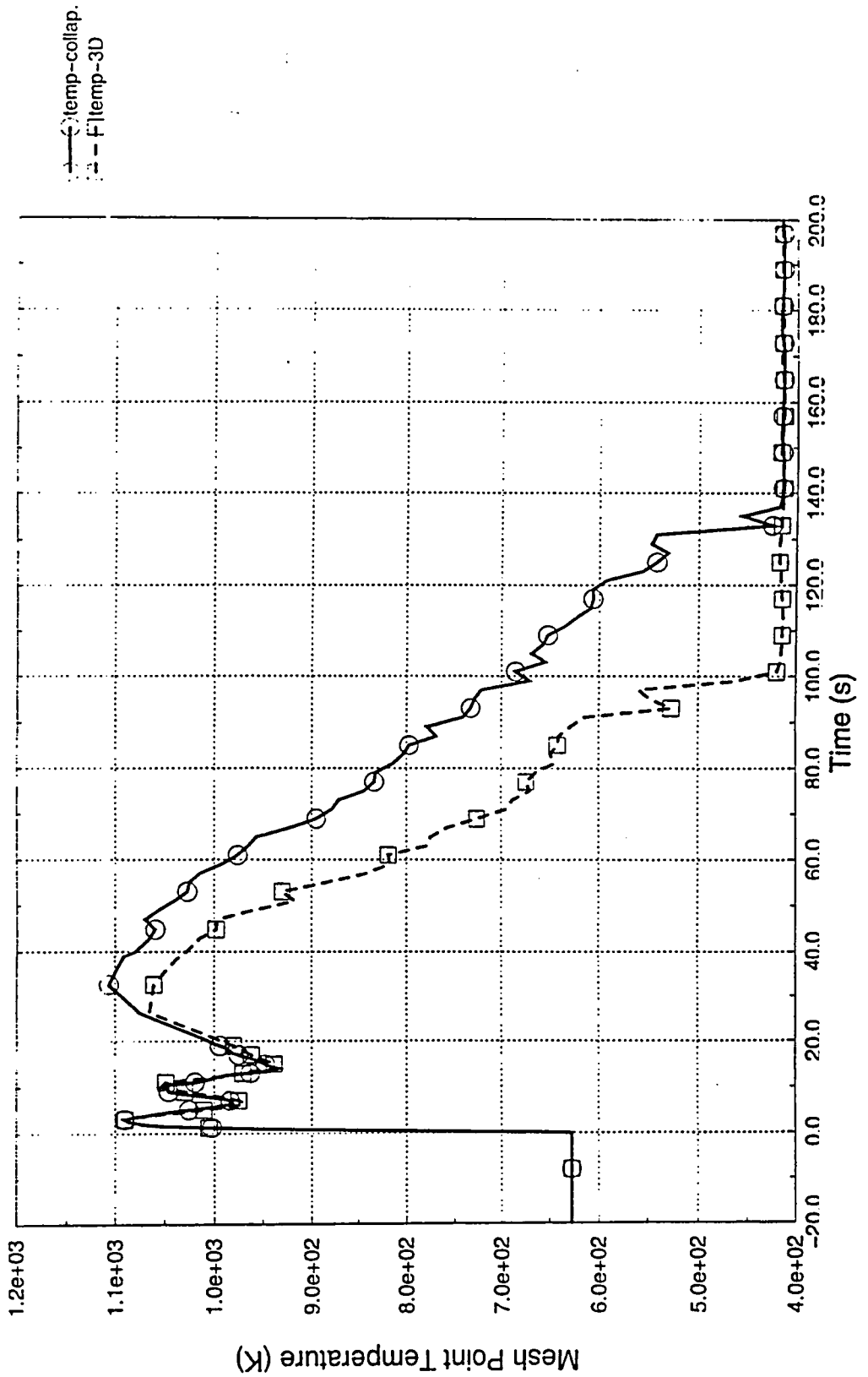

Figure 29. Clad Temperature at Pos. 10 (hot rod)

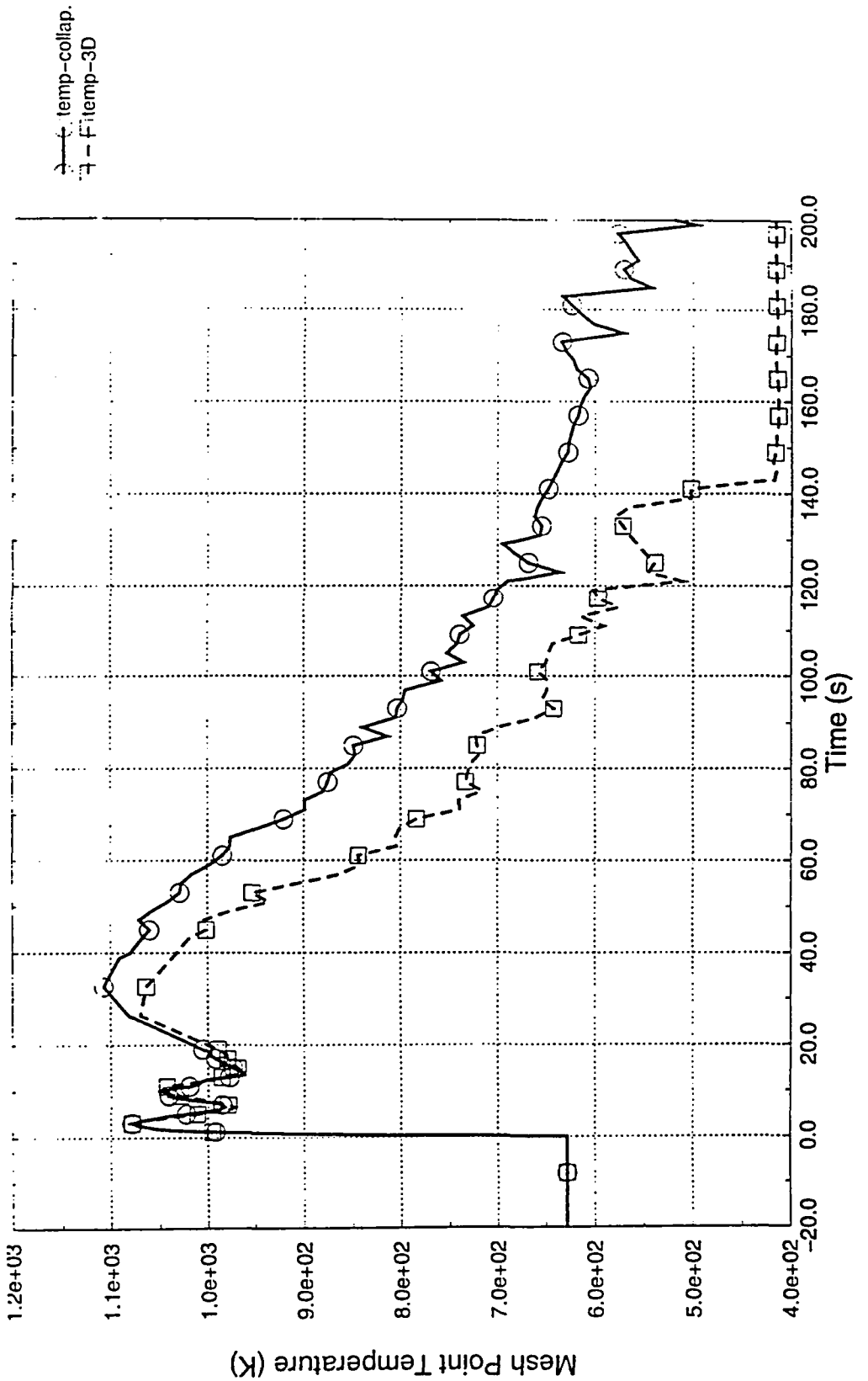

Figure 30. Clad Temperature at Pos. 11 (hot rod)

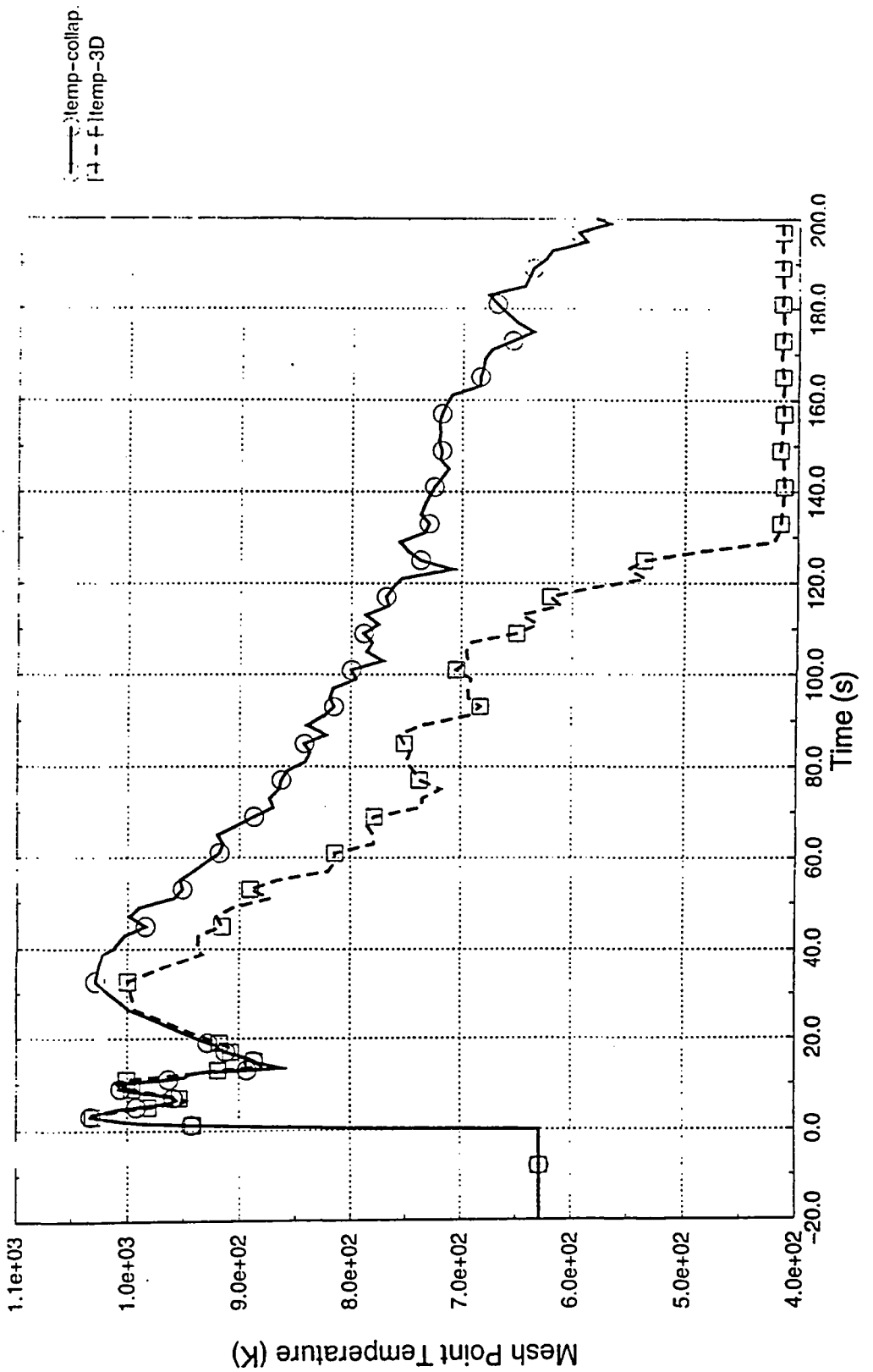

Figure 31. Clad Temperature at Pos. 12 (hot rod)

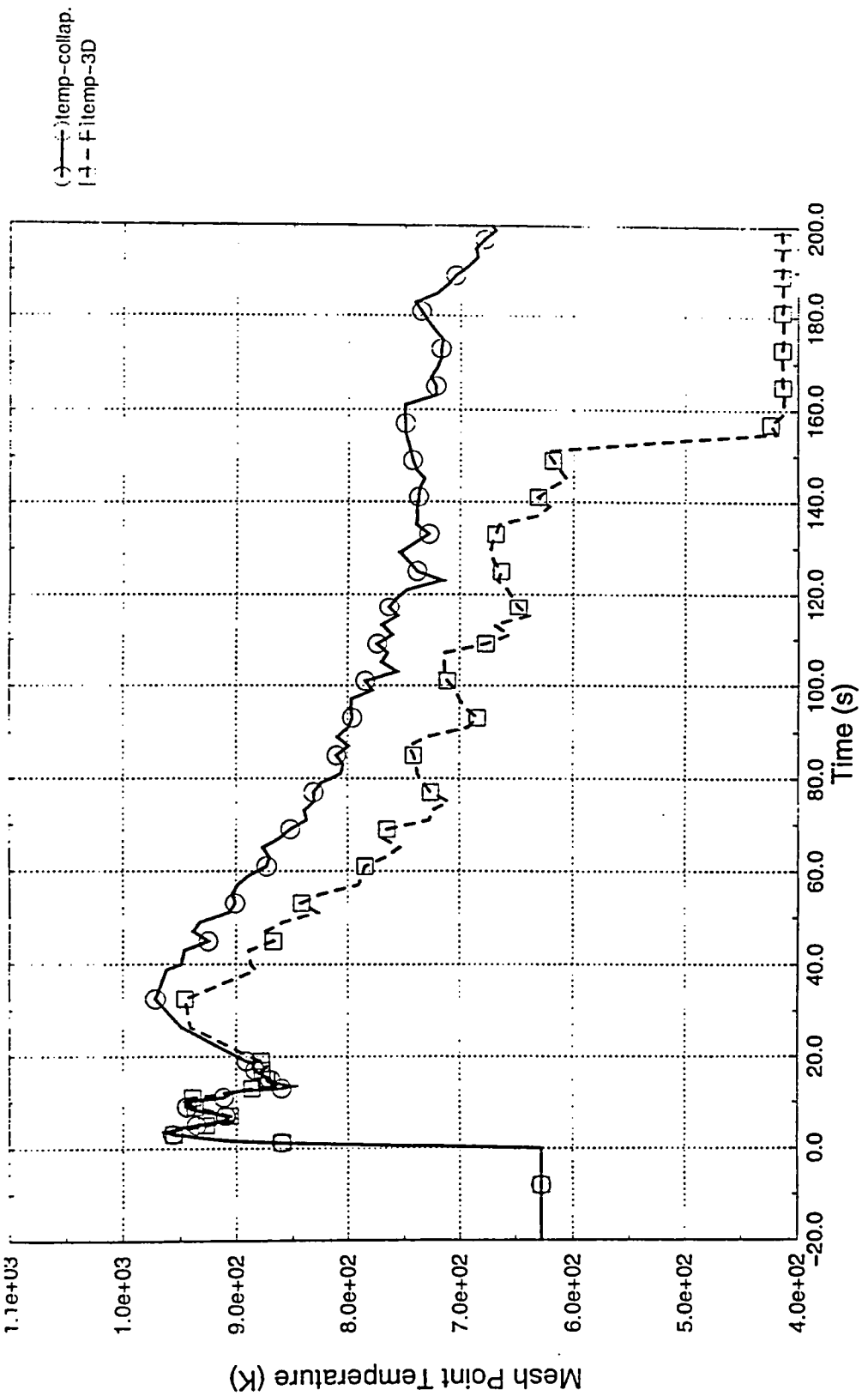

Figure 32. Downcomer Collapsed level. 3D.

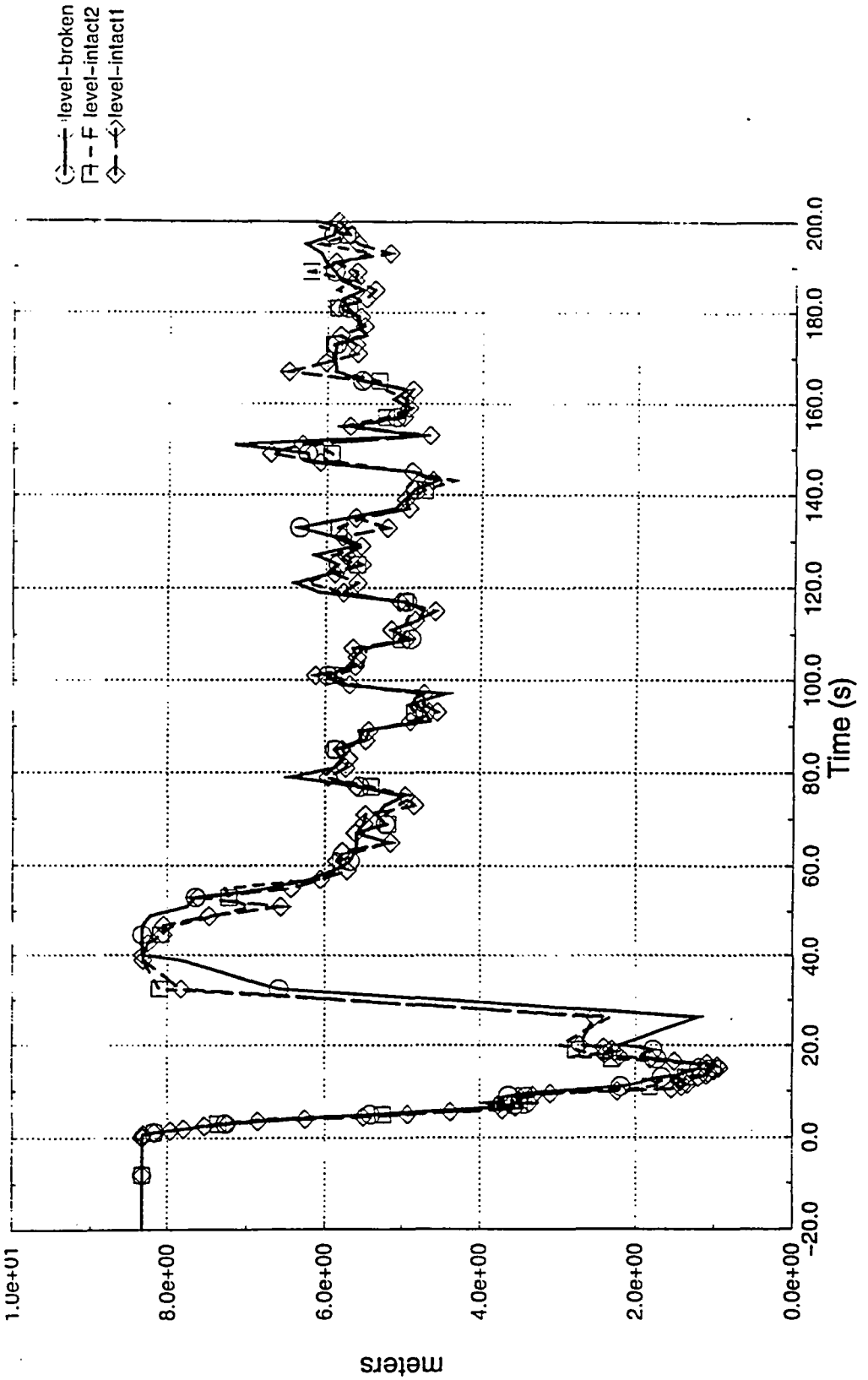

6. CASE 3: REFLOOD MODEL vs. STANDARD HEAT TRANSFER PACKAGE.

In Case 3 two different runs were made. The first run was made with the three-dimensional downcomer model and using the gap conductance model of RELAP5/MOD3.2. Due to the lack of a reflood model in this CAMP version, the second run was made using a development version: RELAP5/MOD3.2fg. This second run was also made using the three-dimensional downcomer modelling, the gap conductance model, as well as the new reflood model provided in this version. Therefore, both runs differ only in the use of the reflood model in the second run (and also, in the code version). Nevertheless, in order to only check the impact of the reflood model, the new models implemented in the beta version (that can be requested by the user via the developmental input card) were shut off.

RELAP5/MOD3.2fg includes the reflood improvements made at the Paul Scherrer Institute (PSI) in Switzerland in RELAP5/MOD3.2 to improve the quench front behaviour during the reactor core reflood portion of the transient. Changes were made to the interfacial drag, interfacial heat transfer and wall heat transfer. If the code user activates "reflood" on word 6 of the heat structure data card, then the code uses these updates.

With the cold fuel dimensions, the gap conductance model calculated for both runs an average fuel temperature in the hot rod at the hottest position (12.9 kw/ft) of 1454.1 K, in good agreement with the steady state fuel design codes used at ENUSA. The hot fuel dimensions obtained in the steady state were $2.2837*10^{-5}$ m in the gas gap and $4.579*10^{-3}$ m in the clad outer radius.

The objective of Case 3 is to strictly compare the effect of the reflood model. A careful review of the comparison between both runs (e.g., using reflood model vs. using the default heat transfer package) shows that the standard heat transfer package is more oscillatory than the reflood model.

The figures labeled with *-ref* show the results obtained with the reflood model. Figures labeled with *-wref* show the results obtained with the standard heat transfer package (without reflood model). Figure 33 through 35 show the core inlet mass flow, core outlet flow, and the collapsed core liquid level. It can be observed that the core mass flow and the liquid amount is very oscillatory without the reflood model. A more detailed review of Fig. 34, for instance, shows that between t = 20 and 40 seconds (just at the beginning of the reflood period), large amounts of water are swept out to the vessel upper plenum in the standard heat transfer package calculation.

The oscillatory hydrodynamic behaviour caused by the standard heat transfer package is produced by the non-smooth behavior of the heat transfer coefficient. Figs. 36 through 38 show the heat transfer coefficient at three different core elevations. It can be observed that large peaks are calculated by the standard heat transfer package in the heat transfer coefficient. This is due to the lack of a heat transfer quench model and a fine renodalization to properly characterize the quench level.

In the standard heat transfer package, heat transfer coefficients in the rewetting zone (film boiling - transition boiling - nucleate boiling) are computed based on the local fluid conditions. In the refllood model, the heat transfer coefficient is also space- dependent. This means that the heat transfer coefficient is gradually forced to decrease in the

transition film boiling regime, upstream of the quench level. This reduction is done by multiplying the heat transfer coefficient obtained with a standard correlation by an empirical factor exponentially dependent on the distance to the quench position.

The exponential reduction of the heat transfer coefficient in the transition film boiling regime is, in concept, based on the stability of the vapor film formed just above the quench front. The continuous steam generation in the quench front causes the formation of a steam film that reduces the heat transfer upstream of the quench front. A large amount of water can exist just upstream of the quench front, but the vapor film precludes a high heat transfer coefficient. The standard package does not take this effect into account, with the heat transfer coefficient dependent only on the bulk fluid conditions.

Figs. 39 through 44 show the cladding temperature at selected core elevations (elev. 7 to 12). The run made with the standard heat transfer package (label *-wref*) and the run made with the reflood model (label *-ref*) calculate similar cladding temperatures at the lower elevations (see Figs. 39 & 40), with the standard heat transfer package calculation being more oscillatory. Nevertheless, at the higher elevations, the results using the reflood model differ from those obtained using the standard heat transfer package. In the run made with the standard heat transfer package, the rewetting is delayed. As can be seen in Fig. 35, for the run made with the reflood model, more water remains in the core at t = 100 seconds from the beginning of transient (because lower amounts of water are swept to the upper plenum).

The clad outer radius is shown in Fig. 45, at t = 200 seconds, in the hot rod for both runs. Due to the different cladding temperatures obtained with the reflood model and the standard heat transfer package, the cladding rupture positions and the clad plastic deformation varies. In the reflood model run, the clad fails at position 10 at t = 21.84 seconds. With the standard heat transfer package, rupture is calculated at t = 21.6 seconds, at elevation 9. The sequence of events and the analysis results are given in Tables 6 and 7, respectively.

Table 6. Sequence of Events (Case 3)

	Reflood model run	Standard HT run
Reactor trip signal	2.0 sec.	2.0 sec.
SI signal generated	3.0 sec.	3.0 sec.
Accumulator injection	11 sec.	11 sec.
End of bypass	18 sec.	18 sec
End of blowdown	26 sec.	26 sec.
Safety injection	26 sec.	26 sec.
Beginning of reflood	28 sec.	28 sec.
Accumulator empties	42 sec.	42 sec.

Table 7. Analysis Results (Case 3)

	Reflood model run	Standard HT run
Peak clad temperature	1190 K	1193 K
Time of peak clad temp.	30 sec.	3 sec.
Peak clad temp. elevation	1.9512 m	1.9512 m
Local oxidation	0.95 %	0.8 %
Hot rod burst time	22 sec.	21.6 sec.
Hot rod burst location	2.43 m	2.187 m

Figure 33. Core Inlet Mass Flow (hot channel)

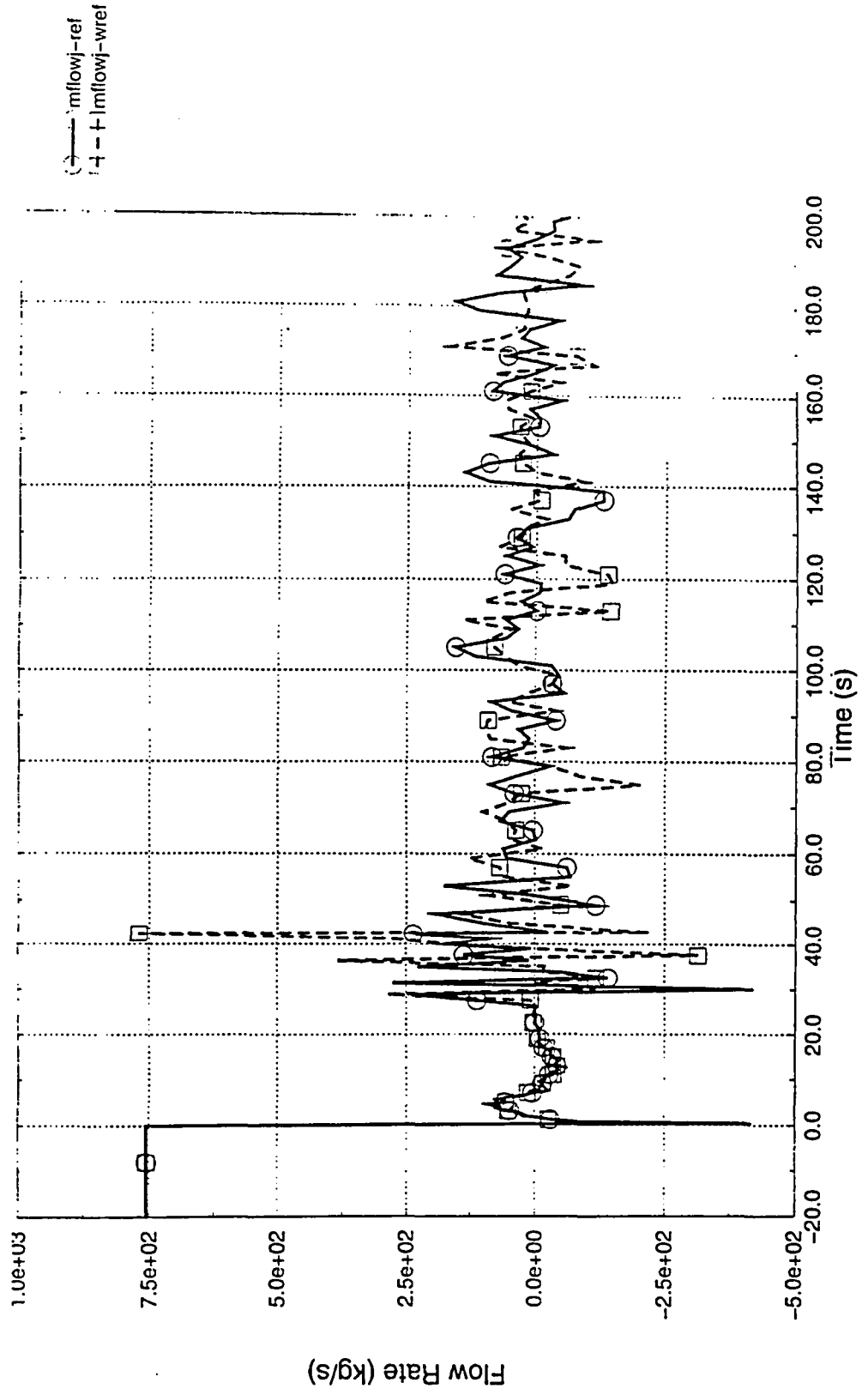

Figure 34. Core Outlet Mass Flow (hot channel)

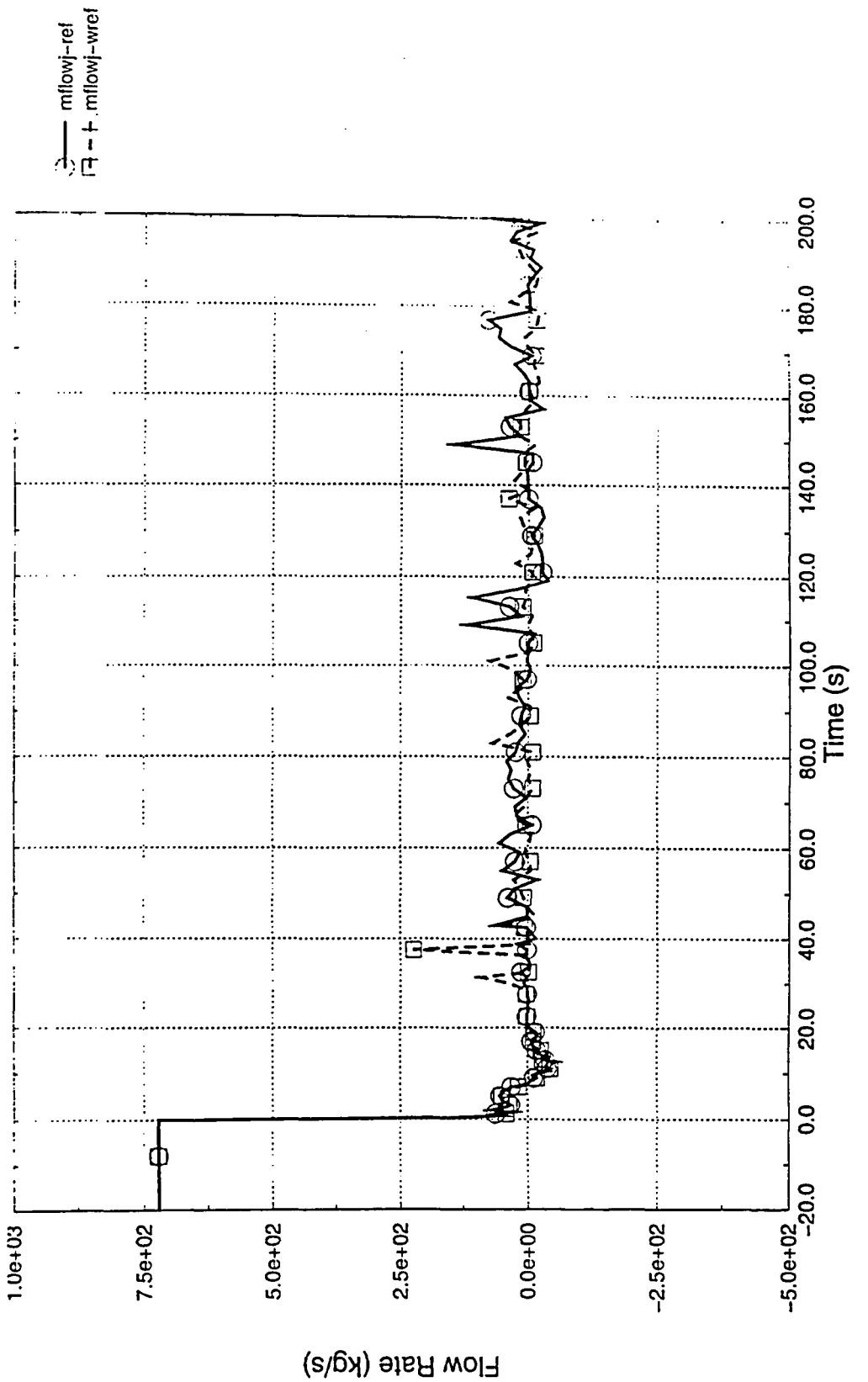

Figure 35. Core Collapsed Liquid Level (hot channel)

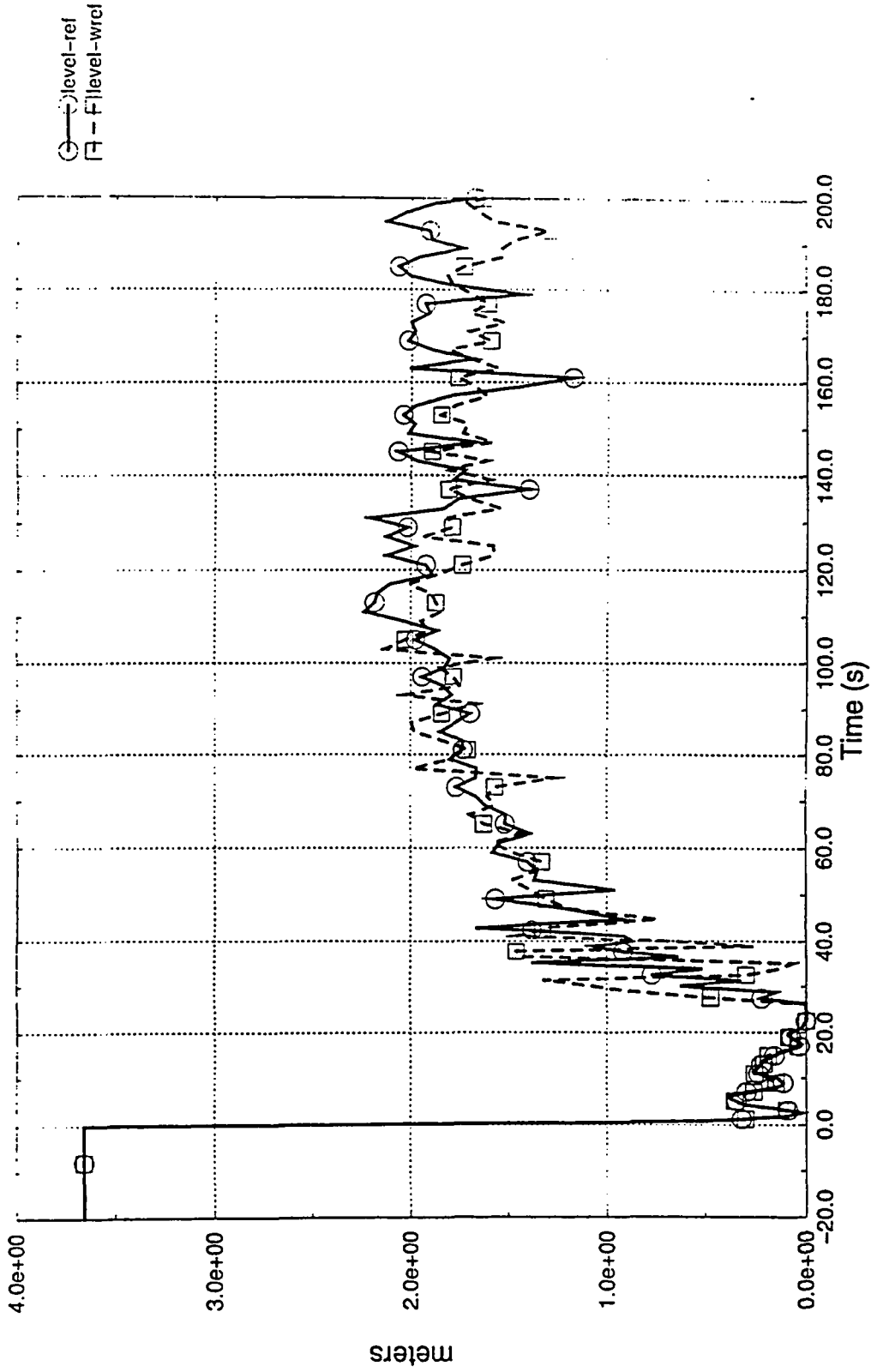

Figure 36. Heat Transfer Coefficient at Pos. 4 (hot rod)

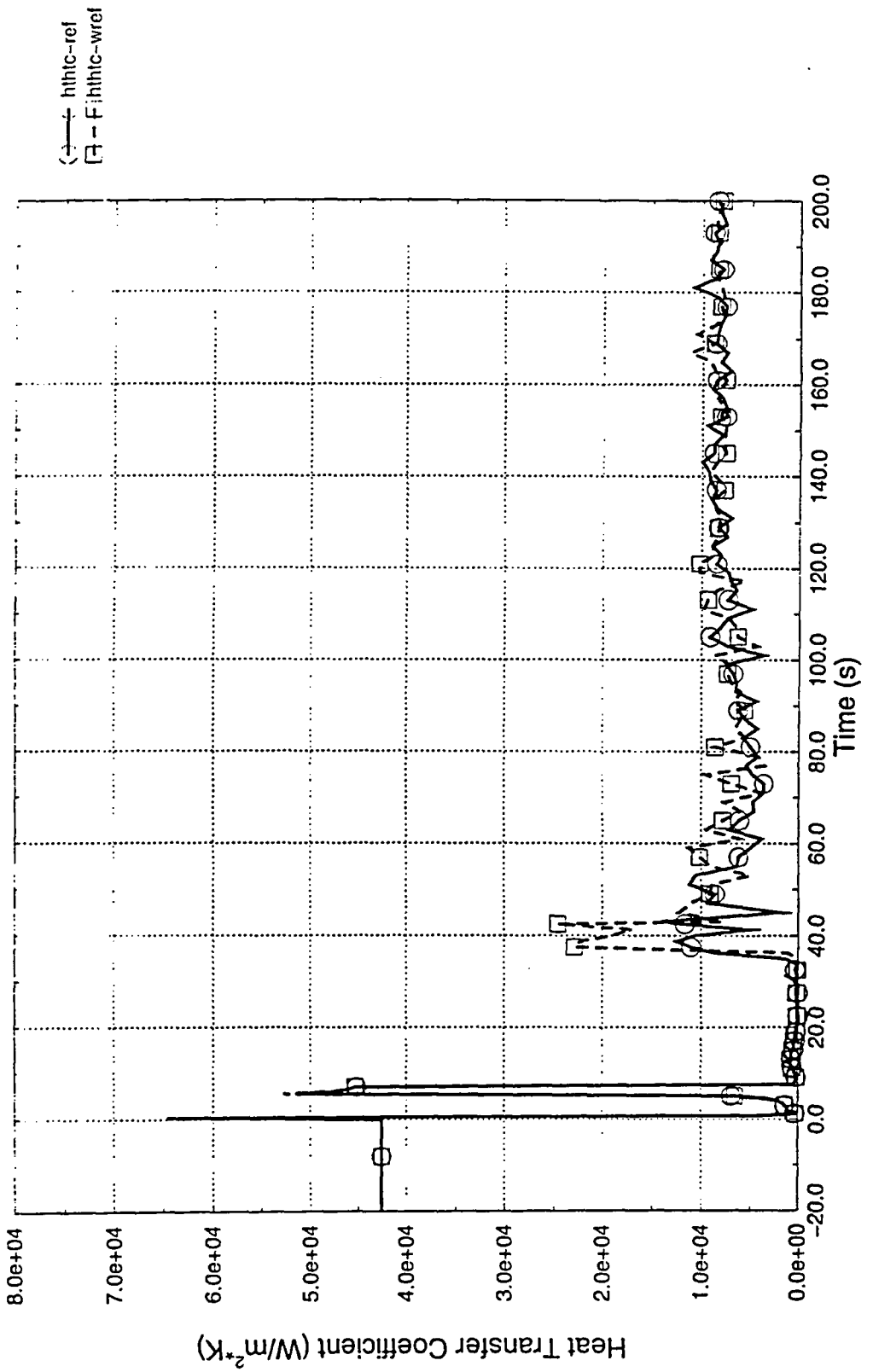

Figure 37. Heat Transfer Coefficient at Pos. 8 (hot rod)

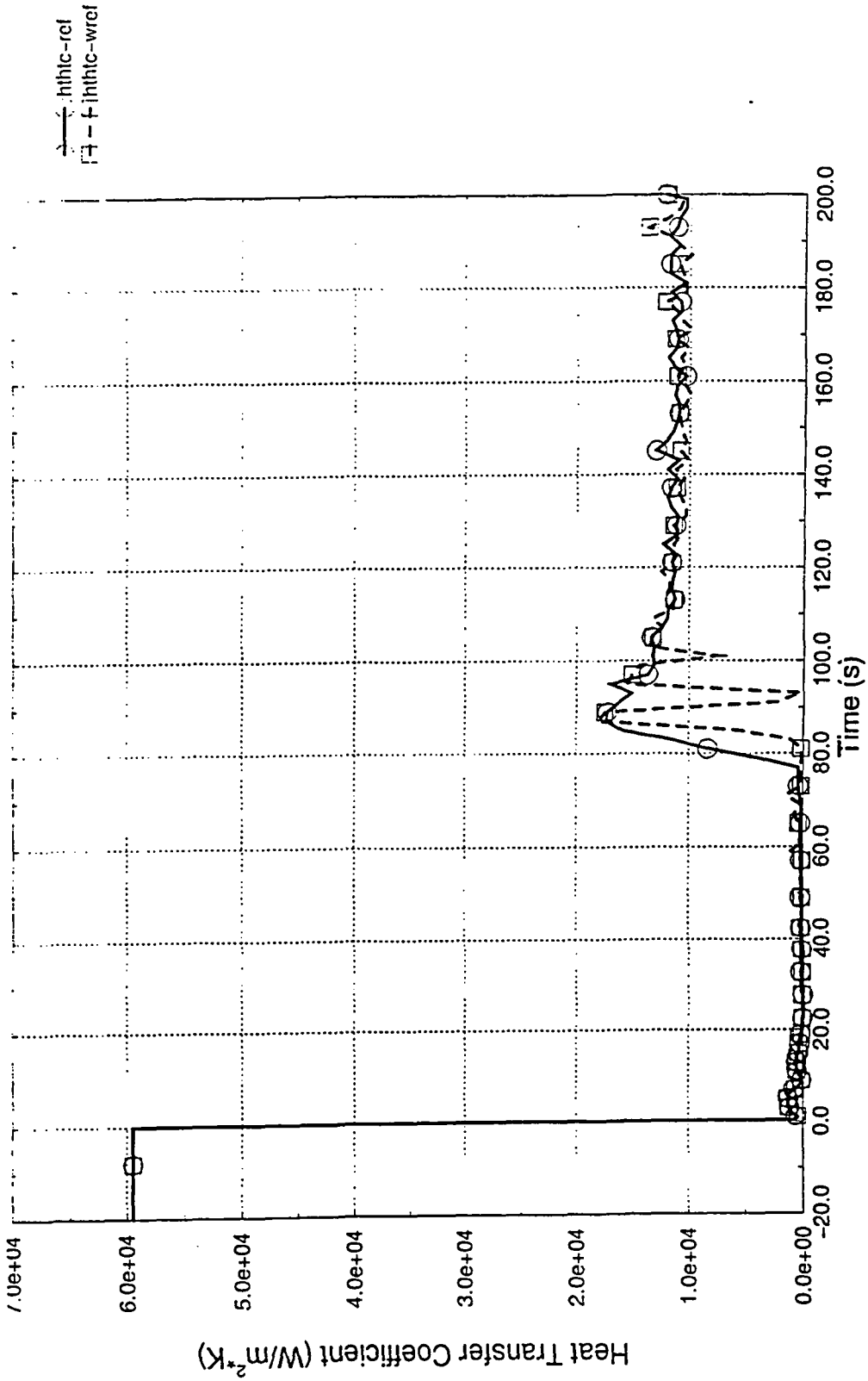

Figure 38. Heat Transfer Coefficient at Pos. 9 (hot rod)

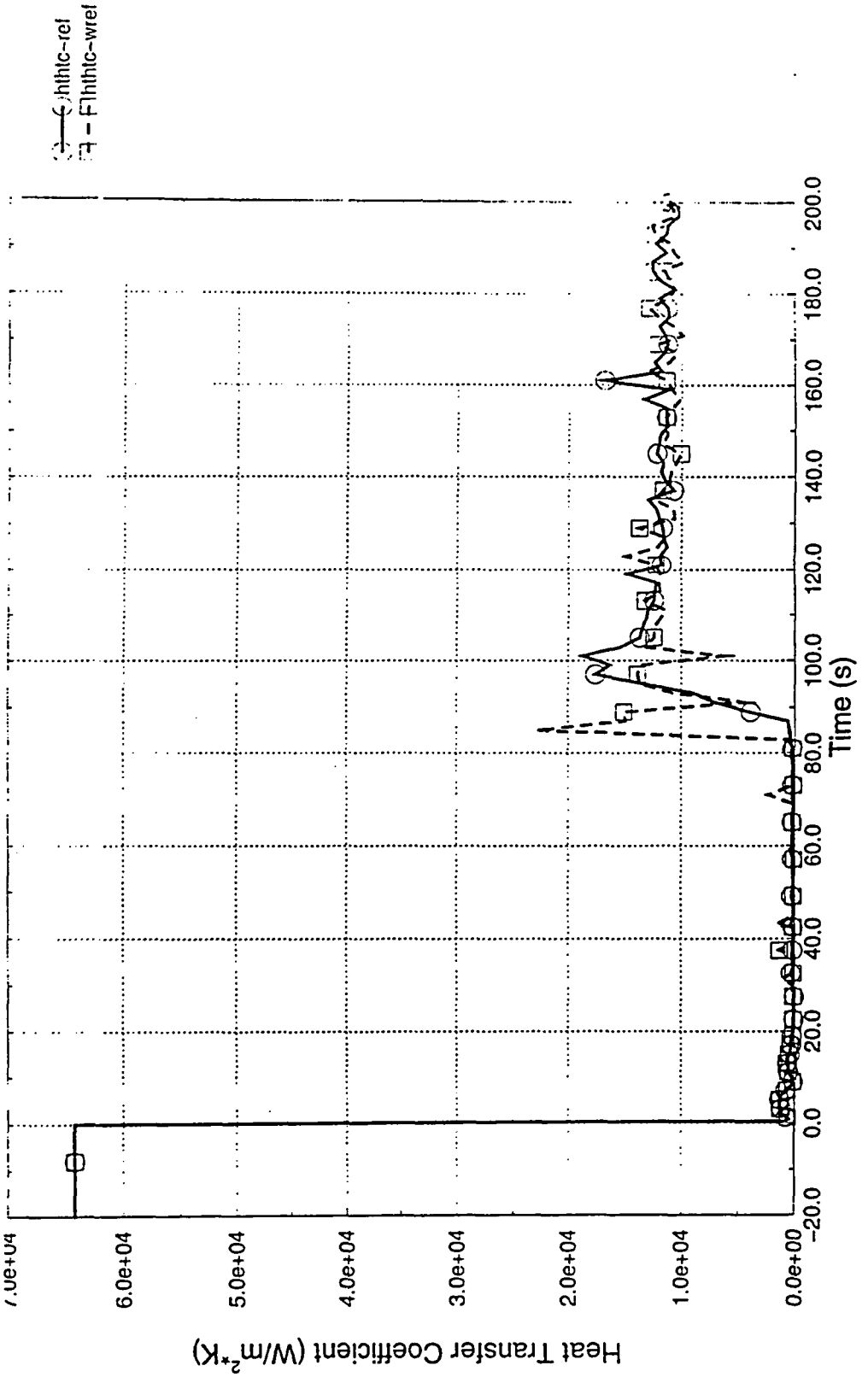

Figure 39. Clad Temperature at Pos. 7 (hot rod)

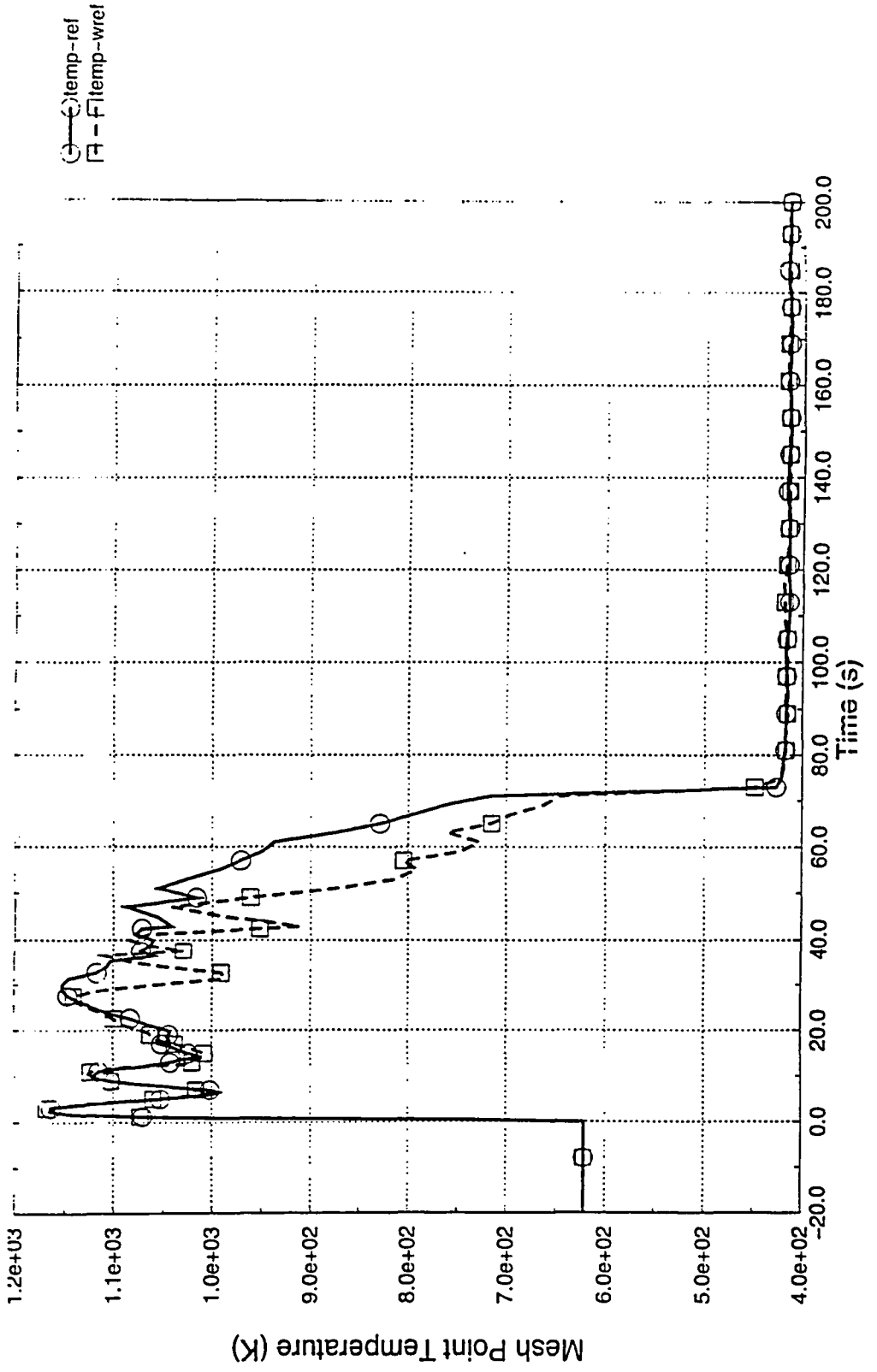

Figure 40. Clad Temperature at Pos. 8 (hot rod)

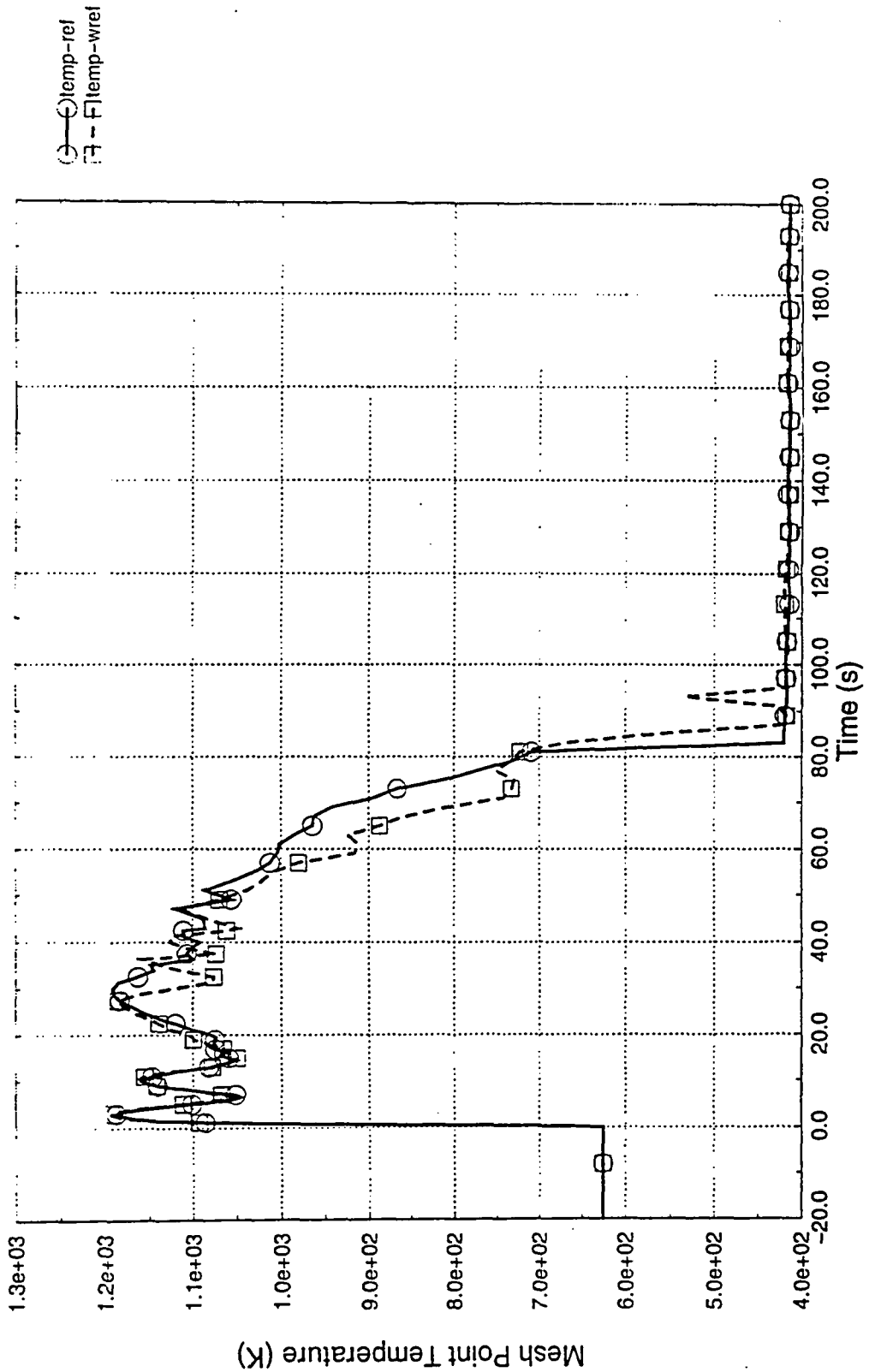

Figure 41. Clad Temperature at Pos. 9 (hot rod)

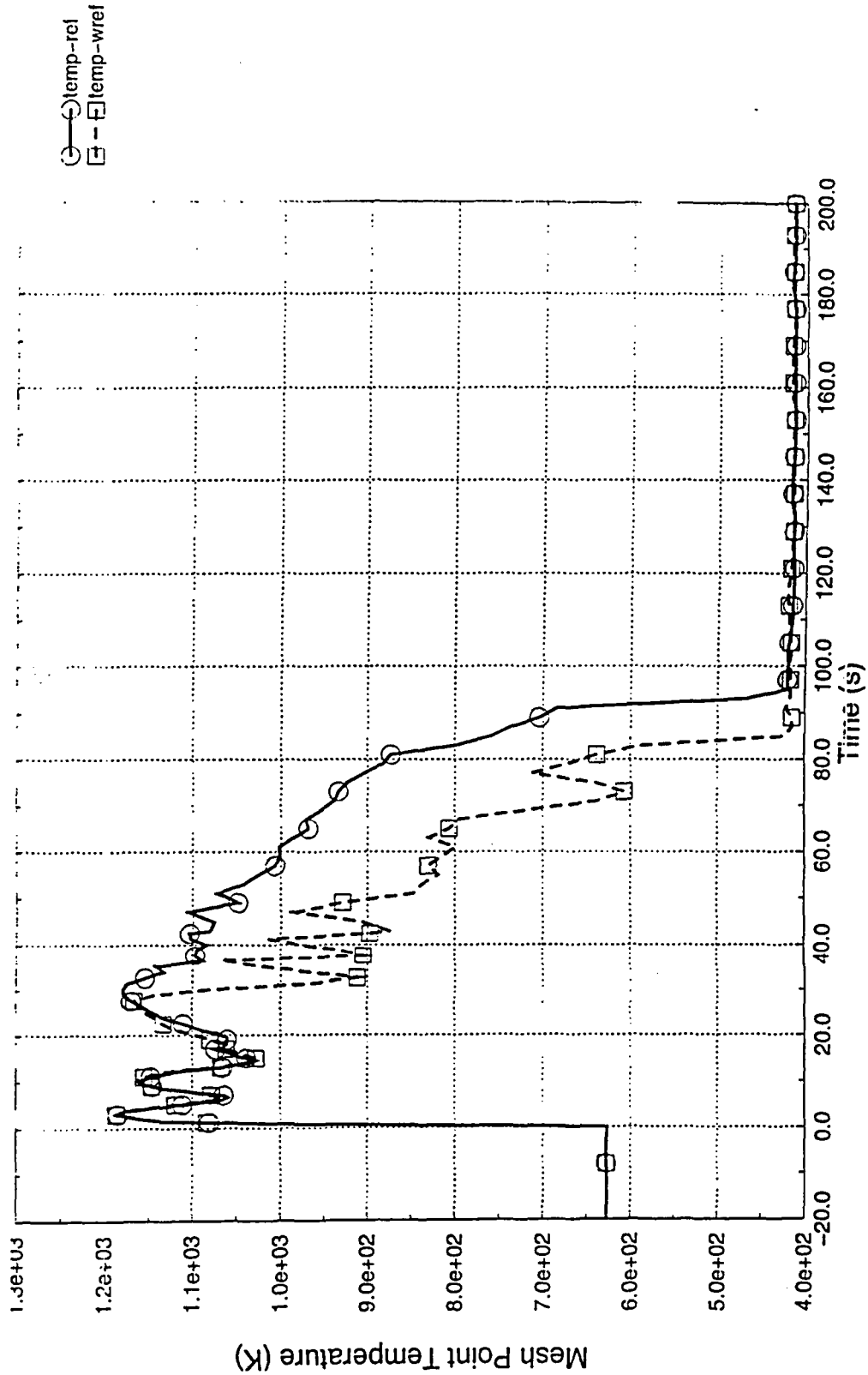

Figure 42. Clad Temperature at Pos. 10 (hot rod)

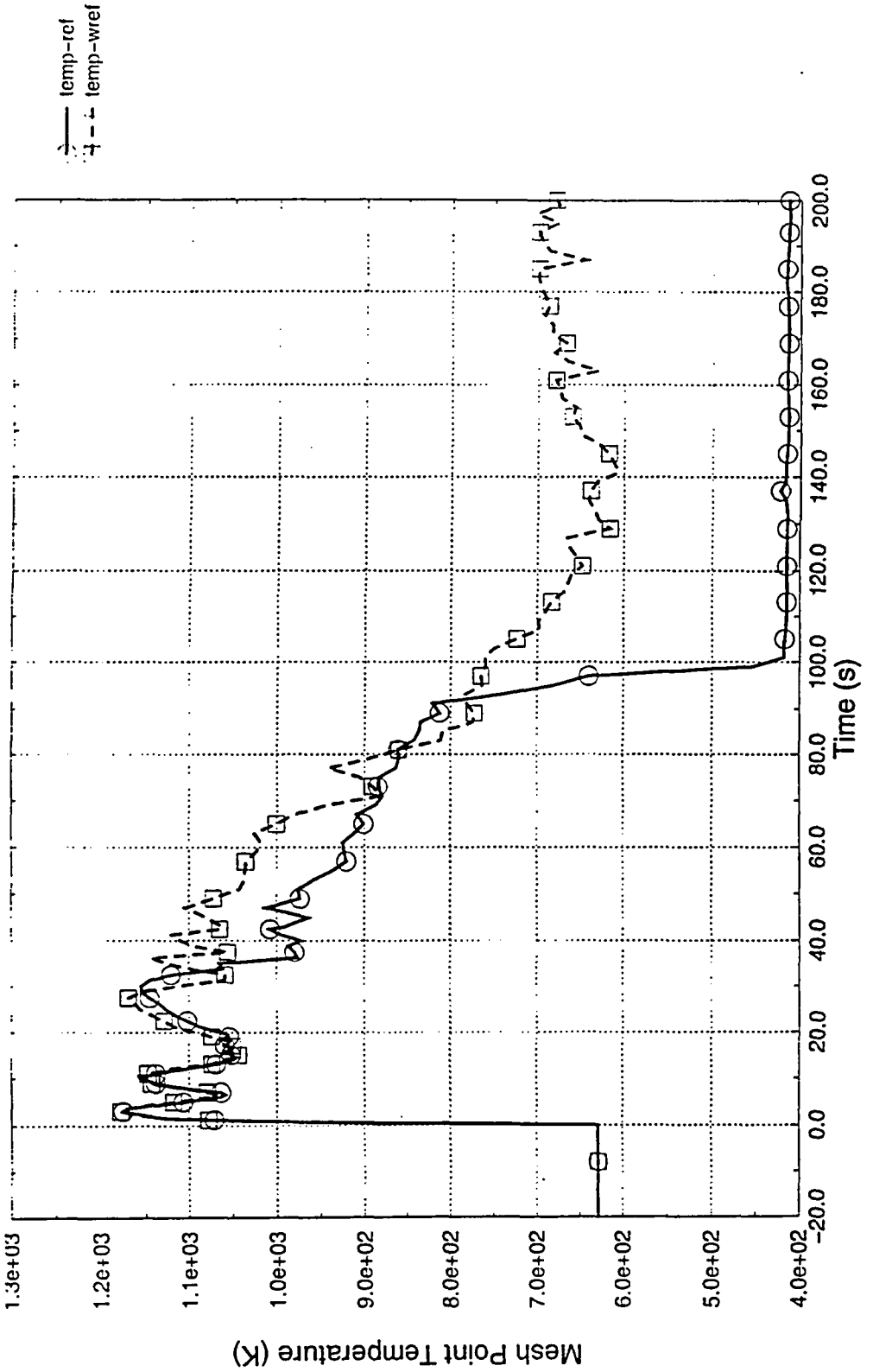

Figure 43. Clad Temperature at Pos. 11 (hot rod)

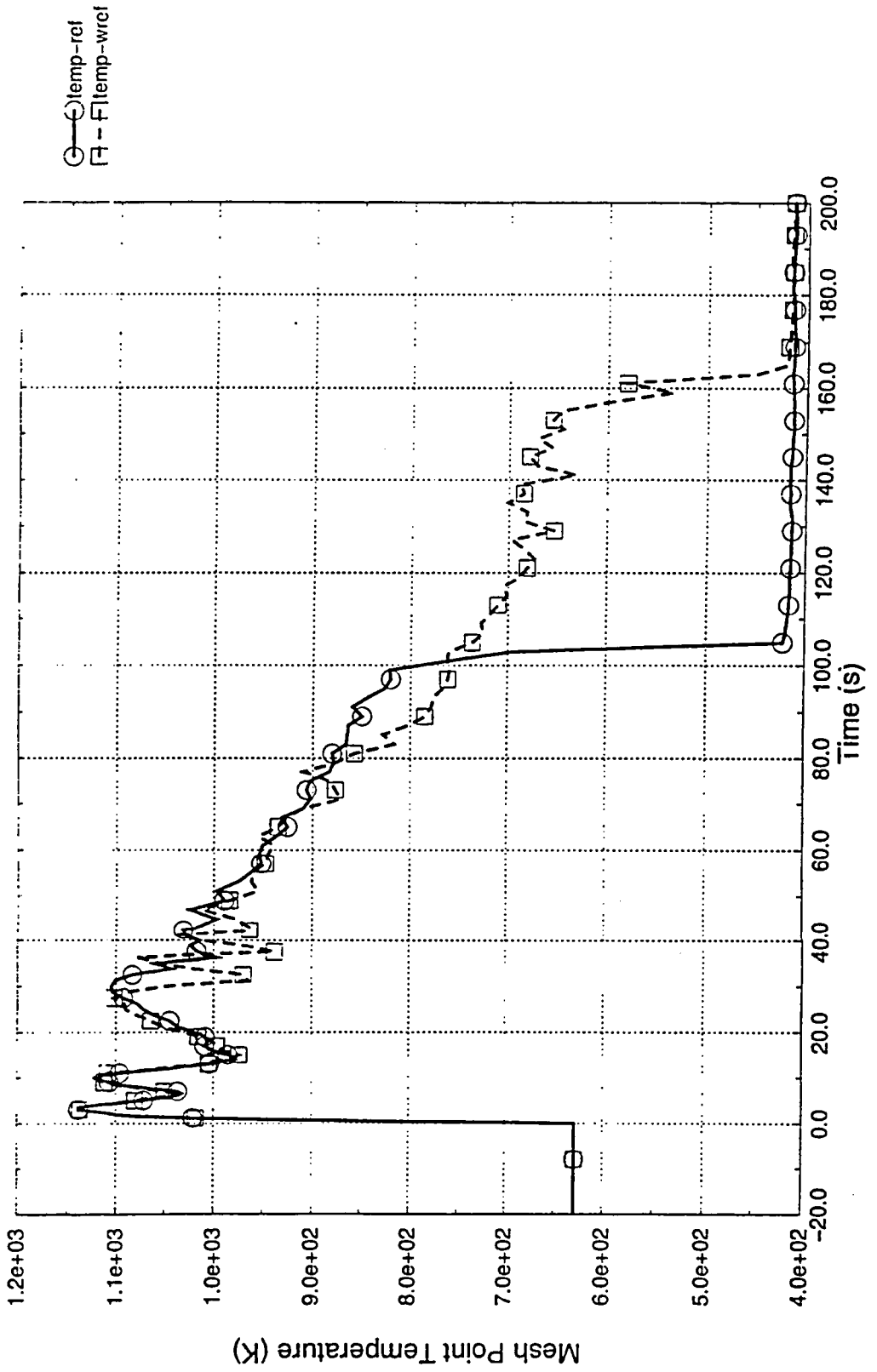

Figure 44. Clad Temperature at Pos. 12 (hot rod)

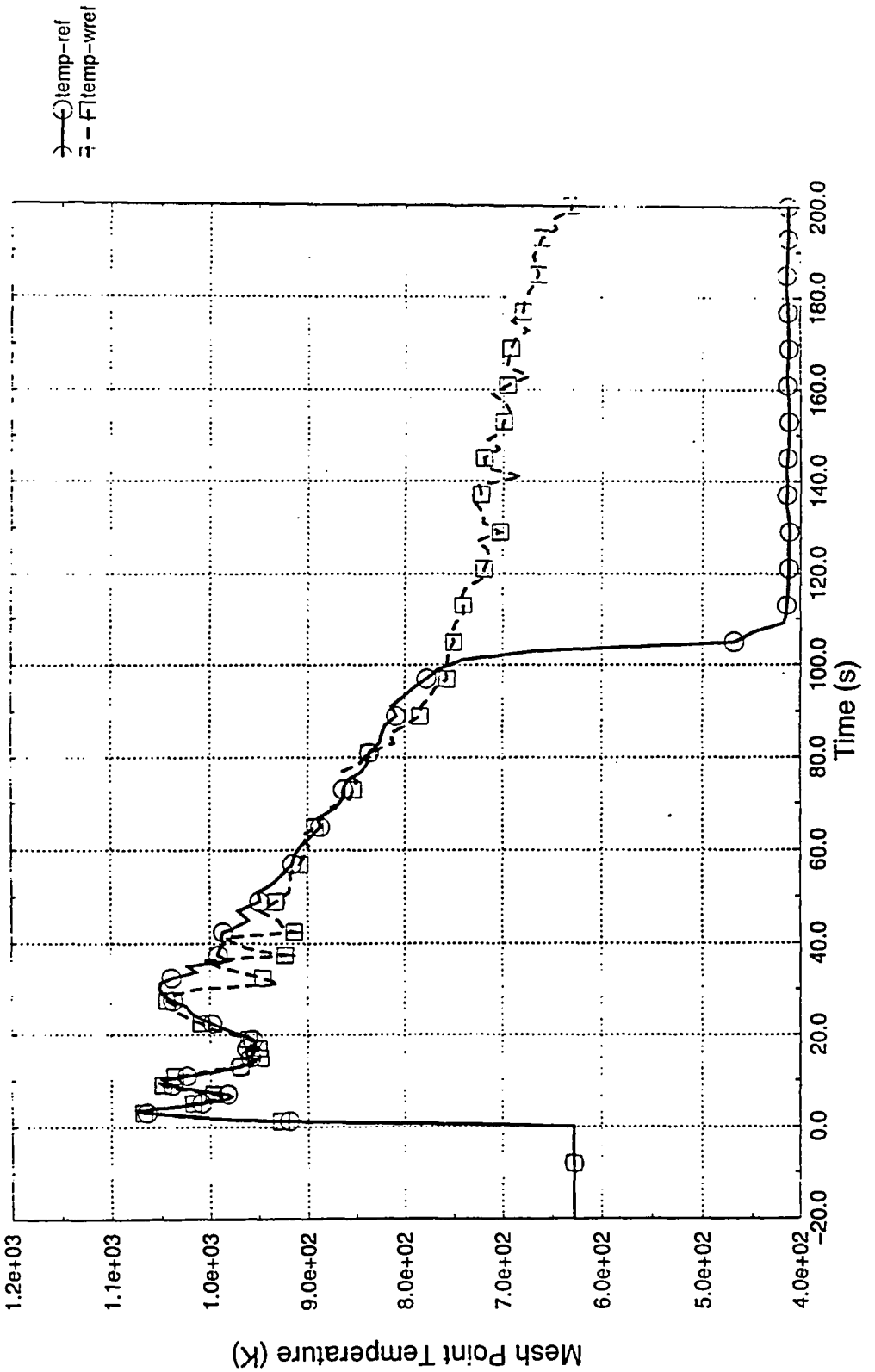

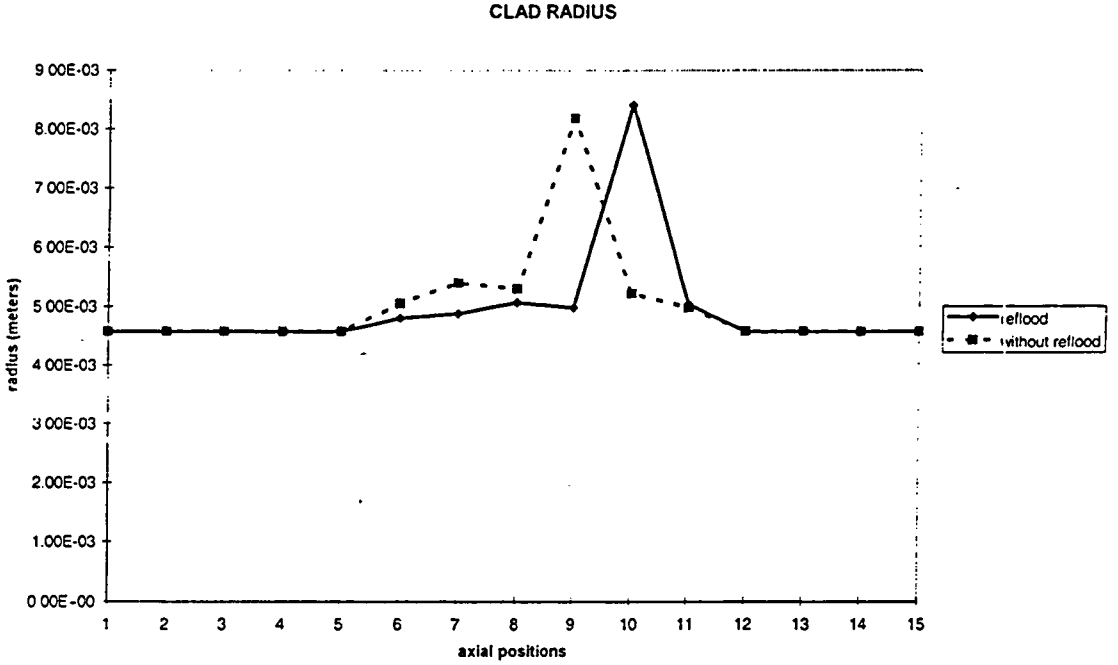

Figure 45. Clad radius (hot rod)

7. RUN STATISTICS

The first case analysed was run both on a CRAY-YMP computer, and on a work-station ALPHA SERVER 4100. The run statistics are given in Table 8.

Table 8. Run statiscs for the first case analysed.

Number of cells	270
Number of time steps (CRAY/ALPHA)	47190/49388
Maximum time step size	0.05 sec.
Problem time	400 sec.
CPU time. (CRAY/ALPHA)	23552/3816 sec
CPU x 1000 / (n vol x n time steps) (CRAY/ALPHA)	1.85 /0.29

The second case analysed was run on an ALPHA SERVER 4100. For this second case, two runs were made, using a downcomer collapsed model in the first and using a three-dimensional downcomer model in the second. The run statistics for these two runs are given in Table 9.

Table 9. Run statistics for the second case analysed.

Number of cells (collapsed/3D)	270/292
Number of time steps (collapsed/3D)	49388/39849
Maximum time step size	0.05 sec.
Problem time	400 sec.
CPU time. (collapsed/3D)	3816/3520 sec
CPU x 1000 / (n vol x n time steps) (collapsed/3D)	0.29/0.30

The third case analysed was run on an ALPHA SERVER 4100. For this third case, two runs were made, using the RELAP5/MOD3.2fg developmental version, with the reflood model activated in the first and the standard heat transfer package of RELAP5/MOD3.2 (CAMP release) used in the second. The run statistics for these two runs are given in Table 10.

Table 10. Run statistics of the third case analysed.

Number of cells	292
Number of time steps (reflood/standard)	33558/43057
Maximum time step size	0.05 sec.
Problem time	400 sec.
CPU time. (reflood/standard)	3411/3887 sec
CPU x 1000 / (n vol x n time steps) (reflood/standard)	0.35/0.31

8. SUMMARY AND CONCLUSIONS

The objectives set forth in Chapter 1 have been accomplished, namely:

- The effect of the downcomer nodalization (collapsed vs. three-dimensional) has been checked.
- The results obtained using the gap conductance model have been compared with those from the steady-state fuel performance design codes used at ENUSA.
- The results obtained with the standard heat transfer package have been compared with the new reflood model implemented in RELAP5/MOD3.2fg (developmental version).
- Two different runs obtained on different computer platforms, using the same input deck, were compared.

The comparison of two identical runs, on two different computer platforms where RELAP5/MOD3.2 was installed , shows the choice of platform to have very little effect on the results for this transient.

The downcomer model, 1-D, 3-D, has an effect on the transient results. In this study, two different downcomer models were compared: a collapsed nodalization downcomer and a three- dimensional nodalization of the downcomer, using cross flow junctions. With the 3-D downcomer model, the ECCS bypass is reduced. The initiation of the reflood period is delayed in the collapsed nodalization compared to the 3-D nodalization model.

Finally, the results show good agreement in the steady-state average fuel temperature when the gap conductance model is used. The comparison made between the standard heat transfer package (RELAP5/MOD3.2) and the new reflood model implemented in the developmental version (RELAP5/MOD3.2 fg) shows the very important effect of this new model on the results. The standard heat transfer package, applied to reflooding phenomena, produces a very oscillatory behavior of the heat transfer coefficients, and consequently, in the hydraulic behaviour as well. The reflood model has a more smooth and reliable behaviour.

All cases analyzed show ample margin to the 10CFR50.46 limits. That is, the peak cladding temperature (PCT) is well below 1477 K (2200 ºF), the maximum local oxidation is bellow 17% of the initial cladding thickness, and the overall hydrogen generation is bellow 1%. A coolable core geometry is maintained, and the long term cooling of the core is assured.

9. ACKNOWLEDGMENTS

This document is a small example of the on-going work being done at ENUSA, related to the validation of the thermal-hydraulics codes. Many people of our organisation have been involved in this project. In particular, the authors want to acknowledge Raúl Arias Orduña, and Marina Trueba Alonso for their special contributions.

10. LIST OF REFERENCES

Ref. 1 INEL-96/005. PSI Reflood Changes for RELAP5/MOD3. Rev. 0. December 1996.

Ref. 2. NUREG/CR-5535. RELAP5/MOD3 Code Manual. June 1995.

NRC FORM 335 (2-89) NRCM 1102, 3201, 3202

U.S. NUCLEAR REGULATORY COMMISSION

BIBLIOGRAPHIC DATA SHEET

(See instructions on the reverse)

1. REPORT NUMBER (Assigned by NRC, Add Vol., Supp., Rev., and Addendum Numbers, if any.)

NUREG/IA-0195

2. TITLE AND SUBTITLE

LBLOCA Analysis in a Westinghouse PWR 3-Loop Design Using RELAP5/MOD3

3. DATE REPORT PUBLISHED

MONTH	YEAR
January	2001

4. FIN OR GRANT NUMBER

5. AUTHOR(S)

J.I. Sanchez, C.A. Lage, T. Nunez

6. TYPE OF REPORT

Technical

7. PERIOD COVERED *(Inclusive Dates)*

8. PERFORMING ORGANIZATION - NAME AND ADDRESS *(If NRC, provide Division, Office or Region, U.S. Nuclear Regulatory Commission, and mailing address; if contractor, provide name and mailing address.)*

Empresa Nacional del Uranio S.A.
Santiago Rusinol, 12
28040 Madrid
SPAIN

9. SPONSORING ORGANIZATION - NAME AND ADDRESS *(If NRC, type "Same as above"; if contractor, provide NRC Division, Office or Region, U.S. Nuclear Regulatory Commission, and mailing address.)*

Division of Systems Analysis and Regulatory Effectiveness
Office of Nuclear Regulatory Research
U.S. Nuclear Regulatory Commission
Washington, DC 20555-0001

10. SUPPLEMENTARY NOTES

11. ABSTRACT *(200 words or less)*

This report documents the analysis of a postulated Large Break Loss-of-Coolant Accident (LBLOCA) in a Westinghouse 3-Loop PWR design analysed using the "Best Estimate" code RELAP5/MOD3. This LBLOCA calculation represents ENUSA's contribution to the "Code Assessment and Maintenance Program" (CAMP). The code used for this analysis is RELAP5/MOD3.2 - the latest CAMP version that was available to ENUSA when this study was performed. Nevertheless, since this version lacked a reflood axial mesh renoding model, a developmental version was also used to analyse the reflood portion of the accident. This developmental version is RELAP5/MOD3.2 fg. Five calculations were analysed, and the results of these were compared. The first case described in this document compares two runs made, using the same input deck, on two different platforms: the CRAY-YMP, and the ALPHA SERVER 4100. Both calculations were done with a basic nodalization: downcomer modelled with one 1-D component (collapsed downcomer), without the gap conductance mode, and without the reflood model. Both cases were run with the original RELAP5/MOD3.2 version. The second case was run to check the impact of modelling a quasi-three-dimensional downcomer, modelled with three 1-D components joined with cross-flow junctions. For the case, the base nodalization used in the first case was modified by adding the new downcomer model, and then compared with the previous results. This case was run on the ALPHA SERVER 4100 with version RELAP5/MOD3.2. Finally for the third case analysed, two additional input decks were prepared. Both of these included the three-dimensional downcomer nodalization and the gap conductance model.

12. KEY WORDS/DESCRIPTORS *(List words or phrases that will assist researchers in locating the report.)*

PANDA
RELAP5/MOD3.2
SBWR

13. AVAILABILITY STATEMENT

unlimited

14. SECURITY CLASSIFICATION

(This Page)

unclassified

(This Report)

unclassified

15. NUMBER OF PAGES

16. PRICE

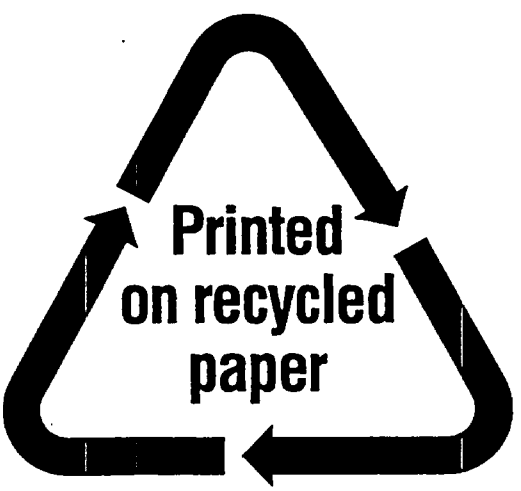

Federal Recycling Program